AD-A043 237 TRACOR INC AUSTIN TEX F/G 17/1
SIGNAL RECOMBINATION STUDIES.(U)
OCT 66 L HALL N123(953)54996A
UNCLASSIFIED TRACOR-66-601-C NL

| OF |
ADA
043237

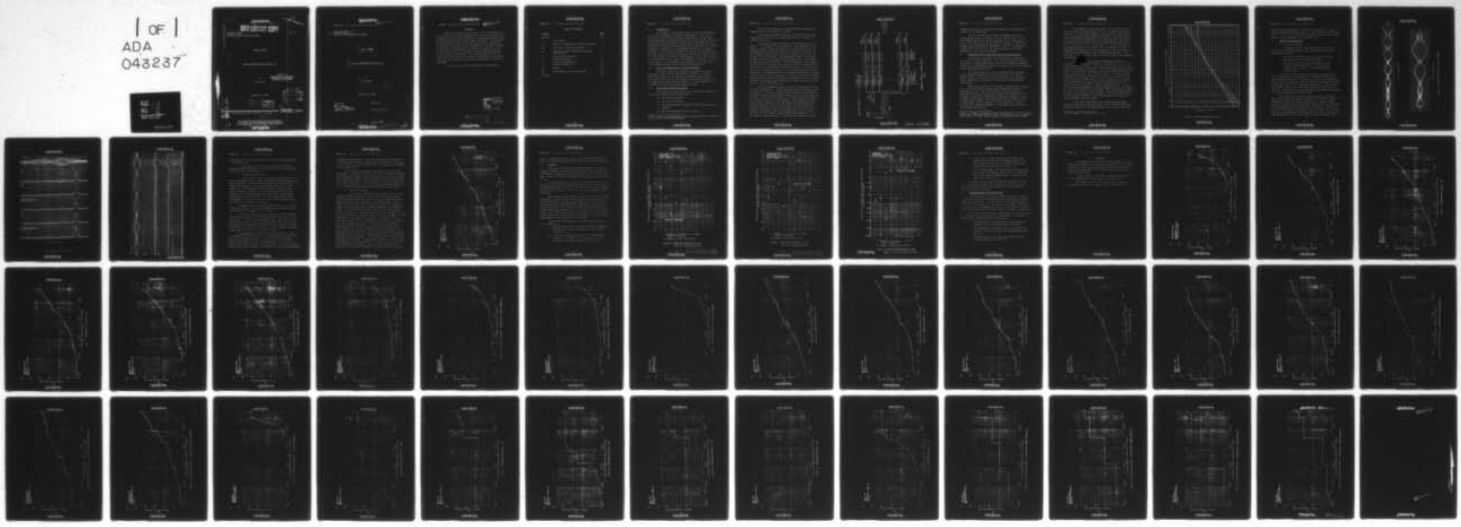

END
DATE
FILMED
9-77
DDC

Document Number
TRACOR 66-601-C
Contract Number N123(953)54996A

FINAL REPORT

SIGNAL RECOMBINATION STUDIES (U)

by

Larry Hall

October 24, 1966

TRACOR INC.
6500 TRACOR LANE • AUSTIN, TEXAS 78721 • 512 926-2800

~~CONFIDENTIAL~~ UNCLASSIFIED

TRACOR, INC. 6500 TRACOR LANE, AUSTIN, TEXAS 78721

(14) Document Number (15)
TRACOR-66-601-C
Contract Number N123(953)54996A

(9) FINAL REPORT,

(6) SIGNAL RECOMBINATION STUDIES (U)

by

(10) Larry Hall

(11) 24 Oct 66 (12) 53 p.

October 24, 1966

Approved:

B M Brown
for A F Wittenborn
Technical Director

Submitted:

Project Director

~~CONFIDENTIAL~~ UNCLASSIFIED

TRACOR, INC. 6500 TRACOR LANE, AUSTIN, TEXAS 78721 UNCLASSIFIED

ABSTRACT

This report contains the results of an investigation of two techniques of signal recombination. This work was directed at improving detection performance in high time-resolution signal processing systems such as the linear correlator. Such systems are susceptible to echo energy splitting and some improvement in detection performance can be expected if a suitable technique is available for recombining the energy in multiple arrivals. In this project, echoes recorded at sea and simulated multiple arrival echoes were analyzed. The results indicate that for these particular echoes, the detection performance of the linear correlator was improved by the signal recombination techniques considered.

A further study of these techniques is recommended.

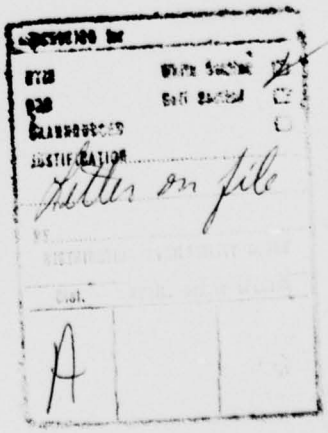

TRACOR, INC. 6500 TRACOR LANE, AUSTIN, TEXAS 78721

TABLE OF CONTENTS

TRACOR, INC. 6500 TRACOR LANE, AUSTIN, TEXAS 78721

I. INTRODUCTION

The purpose of this project was to compare the effectiveness of two techniques of signal recombination. This work was directed at improving the detection performance in high time-resolution signal processing systems such as the linear correlator. Such systems are susceptible to echo energy splitting and some improvement in detection performance can be expected if a suitable technique is available for recombining the energy in multiple arrivals. In this project, echoes recorded at sea and simulated multiple arrival echoes were analyzed. The results indicate that for these echoes, the detection performance of the linear correlator was improved by the signal recombination techniques considered. This project is a continuation and extension of the work reported in the TRACOR document "TASK 8, Signal Recombination"[1].

II. BASIS FOR COMPARISON OF SIGNAL PROCESSORS

The basis chosen for comparison of signal processors is described in full in the TASK 8 report. Briefly, if several processors operate on the same set of signals, the processor which detects one half of the signals at the lowest clutter rate is judged to be the superior processor. In this comparison both recorded sea data and simulated data were used.

III. THE SIGNAL PROCESSING SYSTEMS

Four processors were selected for performance comparison using both simulated and recorded echoes:

(1) The Detector-Averager

(2) The Linear Correlator

(3) The Summed Partial Correlator (SPC) with K parallel channels

(4) The K-overaveraged Linear Correlator

[1] "TASK 8 Signal Recombination," TRACOR Document 66-375-C, submitted under Contract No. N123(953)54996A.

The detector-averager is a power detector and performs independently of coherence in the echo.

The linear correlator provides the best obtainable performance when the echo is a scaled replica of the correlator reference function.

The summed partial correlator block diagram is shown in Figure 1. It consists of K correlators. The reference for the first correlator is the last Kth of the transmitted slide, the reference for the second correlator is next to the last Kth of the transmitted slide, etc., and the reference for the Kth correlator is the first Kth of the transmitted slide. The output of each correlator is delayed appropriately (the ith correlator is delayed by $(K-i)\tau/K$, where τ is the transmitted pulse length) so that all of the signal peaks reach the sum box simultaneously. This processor is the linear correlator when $K = 1$ and the processor is a coherent processor. As K is increased, less coherent processing is available and more incoherent processing is obtained. It is the intent of this processor to effect a compromise between coherent and incoherent processing to recombine as far as possible the energy splitting usually observed in high resolution correlograms of echoes recorded at sea.

The K-overaveraged linear correlator is another technique of signal recombination. When there are resolved multiple arrivals in the echo, the linear correlator performance is determined by the energy in the largest single arrival, not the total energy in the echo. The pulse resolution of this largest single arrival is $1/B$ seconds, where B is the bandwidth of the transmitted slide. In the linear correlator, the rectified correlator waveform is time-averaged over the pulse resolution of the largest single arrival. However, in the K-overaveraged linear correlator, the rectified correlator output is averaged for K times the pulse resolution of the largest single arrival (K/B seconds). It is the intent of this processor to recombine the scattered signal

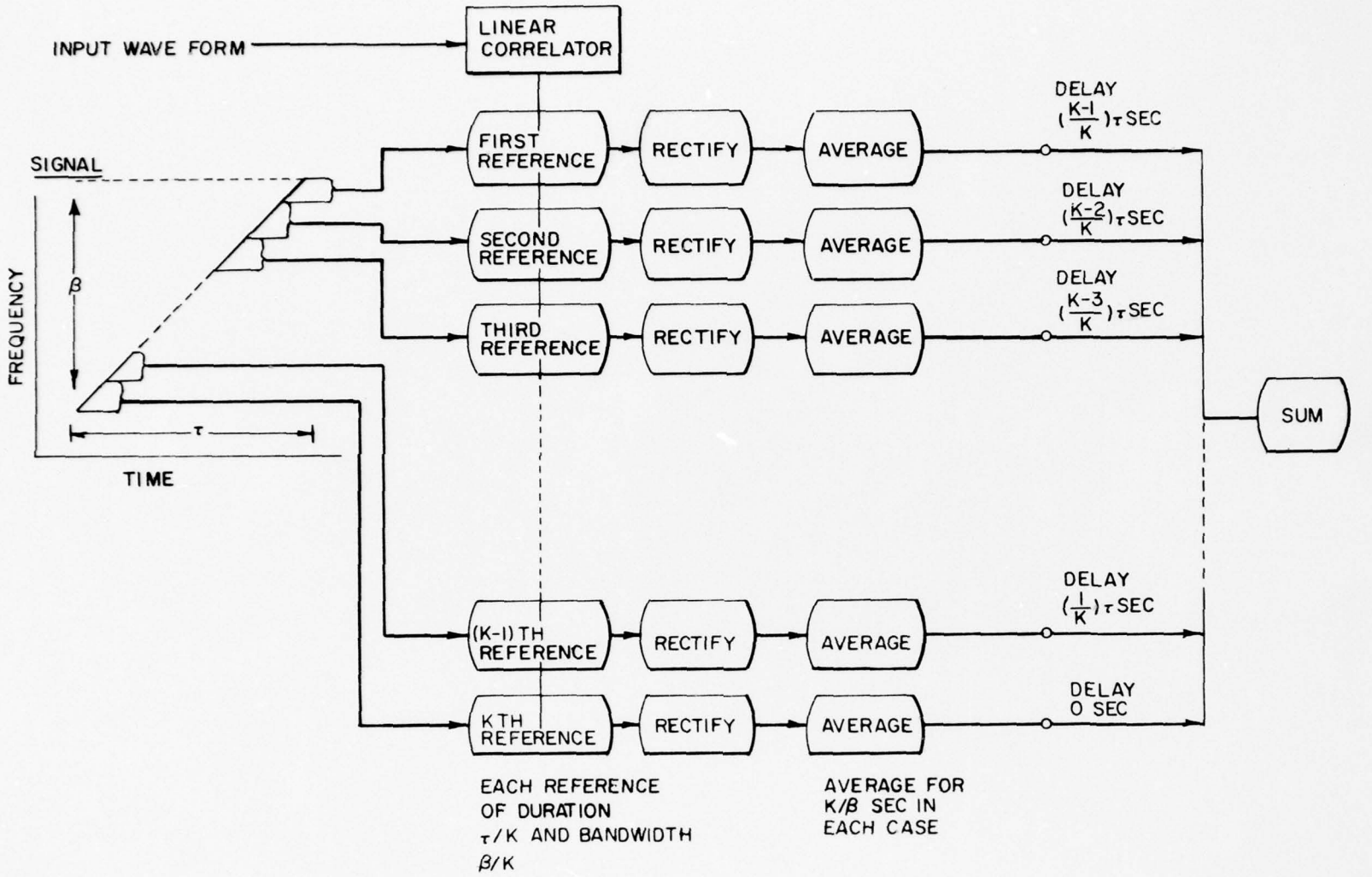

SUMMED PARTIAL CORRELATION

FIG. 1

UNCLASSIFIED

UNCLASSIFIED

3

TRACOR, INC. AUSTIN, TEXAS | 1 DWG 6-25-31 | 4-19-66 BROWN/SL

strength in multiple arrivals by averaging the side regions of energy into a single peak.

In both the SPC with K parallel channels and the K-overaveraged linear correlator, the time resolution at the output is $\frac{K}{B}$ seconds where K is the bandwidth of the transmitted slide. This resolution can be expected to apply as long as any coherent processing gain is obtainable. When K is increased so that $\frac{K}{B} \geq \frac{T}{K}$ or when $K^2 \geq B\tau$, the processing gain is achieved primarily by an incoherent process.

IV. PROCESSOR OUTPUT STATISTICS AND NOISE MARKING RATE

The waveform statistics for noise alone is well-known for two of the four processors. The linear correlator output is described by the Rayleigh distribution and the detector-averager output with time-bandwidth product in excess of 30 is well described by the Gaussian distribution[2].

The output statistics of the summed partial correlator with K parallel channels were fully developed in the TASK 8 report, where it was shown that the distribution at the output can be obtained by K successive convolutions of the Rayleigh distribution.

The output waveform of the linear correlator has correlation time (time between statistically independent samples) of approximately 1/B. Since this waveform is described by the Rayleigh distribution, the output waveform overaveraged by K is obtained by summing K statistically independent samples to form a single output sample. The distribution at the output of the K-overaveraged linear correlator is thus identical to that of the SPC with K parallel channels - K successive convolutions of the Rayleigh distribution.

---

[2]Peter B. Brown, "A Comparison of the Performance of Several Signal Processors," TRACOR Document 66-203-U, submitted to C.O., and Director USNEL, March 10, 1966, under Contract No. N123(953)53354-A NPOLA.

The probability that noise alone will exceed the threshold for each of the processors is shown in Figure 2 plotted as a function of threshold relative to the processor output mean in units of processor output standard deviation. The curve marked 1 is the Rayleigh distribution, the curves marked 2 and 32 are the probability distribution for the summed partial correlator for K = 2 and for K = 32. Curves for K = 4, 8, and 16 have also been obtained but are not shown. The curve marked ∞ is the probability distribution for very large K; it will also apply to the detector averager for large time-bandwidth product. This curve (K = ∞) is a straight line on this grid and is the Gaussian distribution.

Let us suppose that output signal peak of size x is observed from a particular processor. The quantity $T = (x - \mu)/\sigma$ will be computed, where μ is the output noise mean and σ is the noise output standard deviation. T^2 is the output signal-to-noise ratio. In order that this peak will mark the display the detection threshold must be set no higher than T. If this limiting threshold had been the threshold at the time of arrival of the signal, then the probability p_k of noise marking of the display on a particular noise sample is given for this processor by Figure 2 (or its extension to higher thresholds) at T. In this way the minimum probability of noise marking at which each signal can still be detected can be obtained. The signals were processed by each of the processors and a matrix of clutter probabilities p_k was prepared arranged in rows labeled with the k value and columns labeled with echo number.

It has been established* that processor performances should be compared at the same clutter rate. Clutter rates were estimated for each of the probabilities in the matrix described

*See for example P. B. Brown, loc. cit.

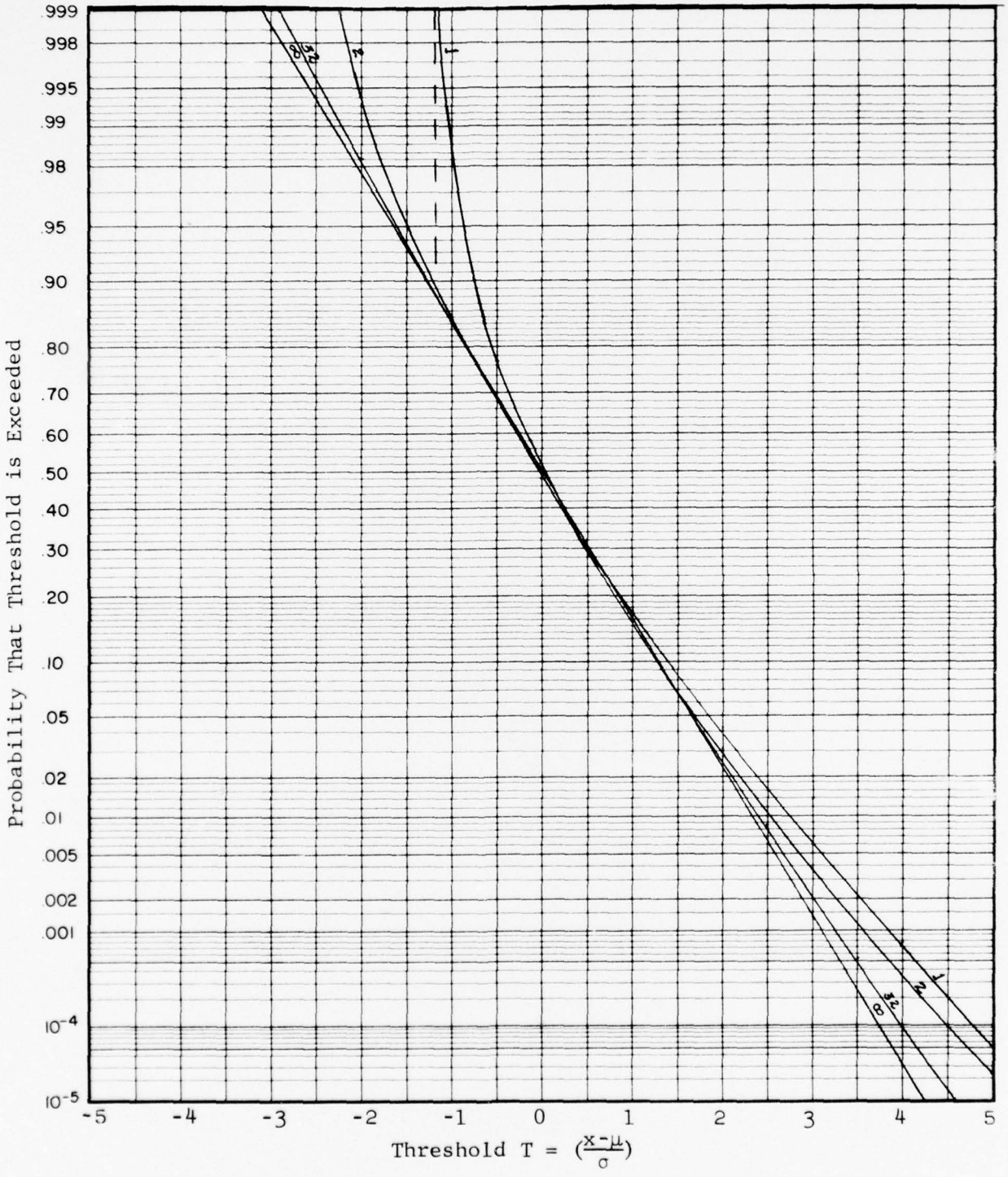

Figure 2 Processor Waveform Statistics

in the previous paragraph. The rate of occurrence of clutter marks is approximately $B \cdot p_k$, where B is the processor output bandwidth. A clutter rate matrix was prepared using this relationship between clutter probability and clutter rate.

V. PROCESSING DESCRIPTION

a. Artificial Signals

A multiple-arrival pulse was chosen as the pulse form for the simulated echoes. The multiple-arrival echo was simulated as follows:

1. a 175 c/s linear FM slide of 1 second duration was generated (the transmitted pulse),
2. two replicas of this slide were added to the original slide with delays of 5 ms and 20 ms respectively to produce the simulated triple arrival echo.

A multiple-arrival echo was similarly produced with a 350 c/s FM slide of 1 second duration. Examples of these pure echoes appear in Figure 3. Ninety such echoes were produced for each of the two bandwidths and were hidden at equispaced intervals in Gaussian noise of the corresponding bandwidth. These signals were hidden in the noise at an input signal-to-noise ratio of -9.0 dB. In addition, the same process was performed with signals of +10.0 dB input signal-to-noise ratio.

The signals were then run through the four processors. The +10 dB signals were easily visible in the processor output waveforms and Figure 4 contains examples of a typical signal output for several of the processors. Since a time correspondence was maintained between the +10 and -9 dB signals, a signal peak for the -9 dB signal was extracted from the waveform at the time that the corresponding +10 dB signal peak occurred. The mean and standard deviation of the noise alone for each processor were

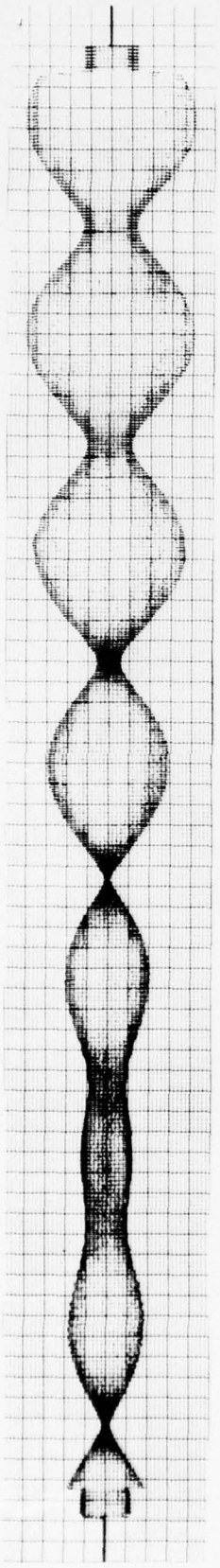

350 c/s Bandwidth

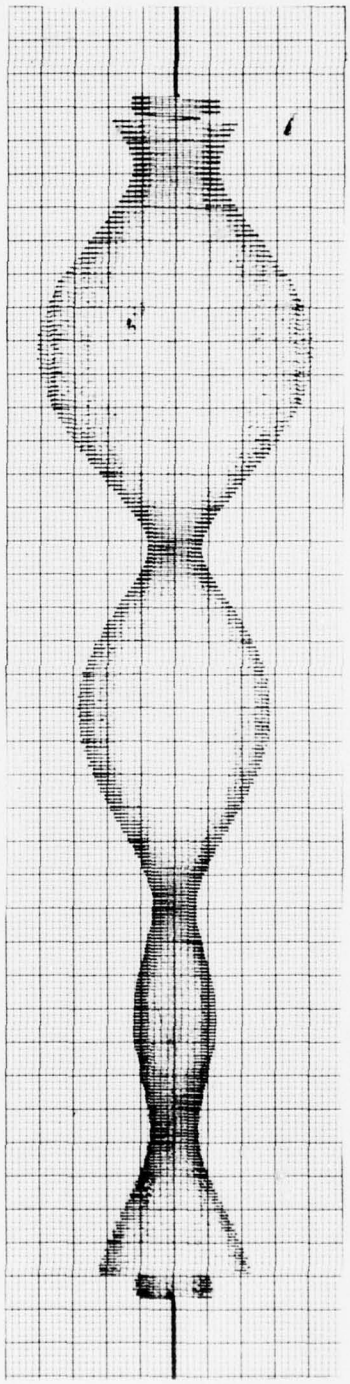

175 c/s Bandwidth

Figure 3 SIMULATED MULTIPLE ARRIVAL ECHOES

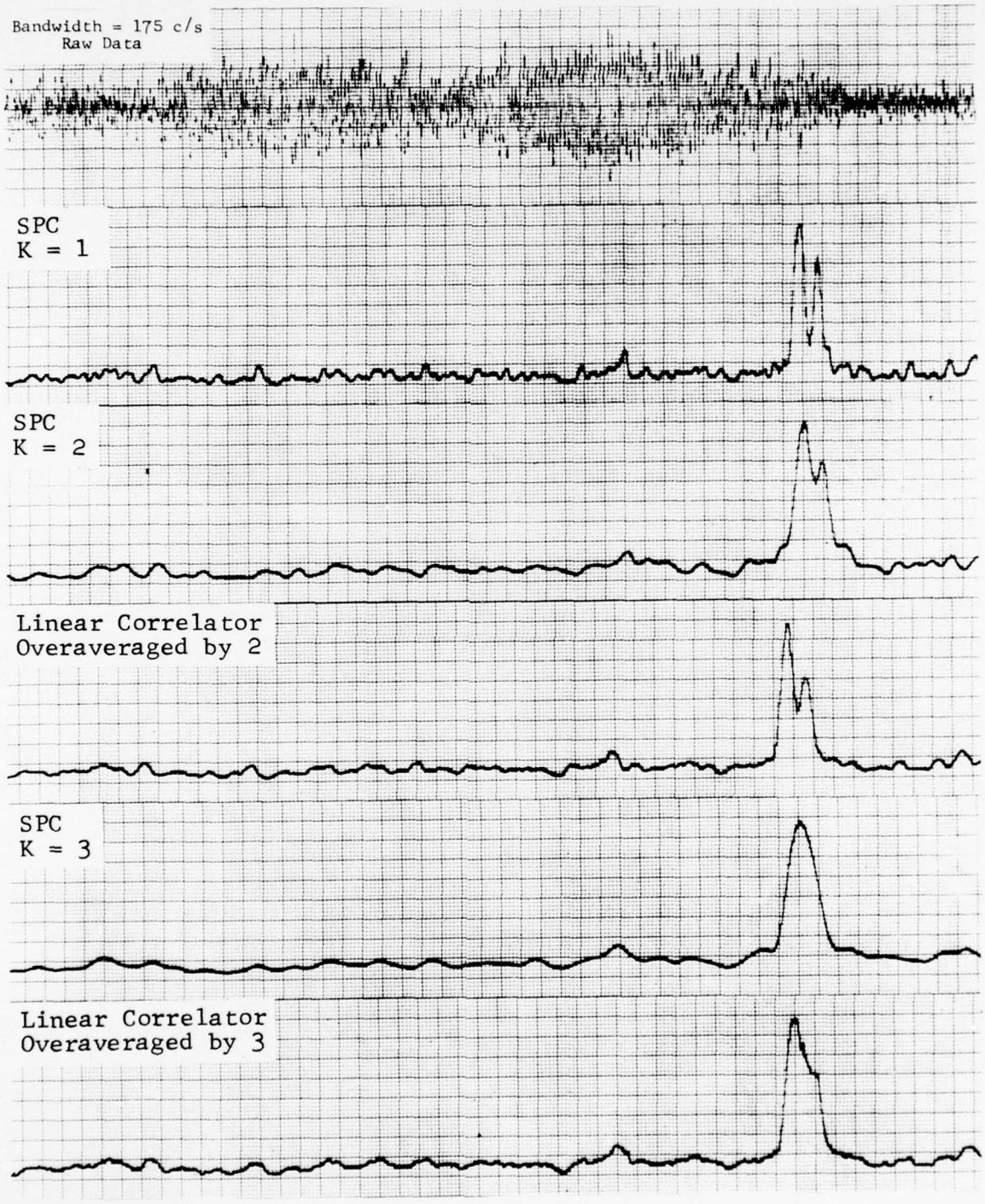

Figure 4 OUTPUT WAVEFORMS OF SEVERAL PROCESSORS

Figure 4 OUTPUT WAVEFORMS OF SEVERAL PROCESSORS (CONT'D)

determined from the output waveform of that processor operating on the noise alone.

In this manner, for each set of ninety, -9 dB input signals of each bandwidth, a set of ninety values of peak minus mean over sigma was obtained.

b. Signals Recorded at Sea

In the task 8 report, the echoes considered were of such large amplitude that their corresponding clutter-rate curves were unrealistic, involving probabilities of the order 10^{-15}. To obtain more realistic data, the recorded echoes used in this project were of relatively small amplitude. Seventeen echo cycles recorded at sea with FM slide transmissions of 200 c/s bandwidth and 1 second duration were analyzed. An additional seventeen echo cycles with 400 c/s, 1 sec transmissions were investigated. For each echo cycle, the recorded transmit pulse was used as the correlator reference.

The signals were run through the SPC with 2, 3, 4, 6 and 8 parallel channels. The K-overaveraged linear correlator was run with values of K equal to 2, 3, 4 and 5.

For each processor, a printout was obtained of the amplitude and time location of the 25 largest peaks in each of the 17 echo cycles. In the 175 c/s bandwidth case, a peak from the four processors occurred at the same range in each of the echo cycles. No consistency in peak position was observed in the 400 c/s bandwidth data for any of the processors. It was concluded that these signals were too small for successful analysis.

The signal peaks obtained were then converted to values of T described in section IV (i.e. T equals peak minus noise mean over noise standard deviation). The noise mean and standard deviation for each echo cycle were obtained from two sections of noise lying on either side of the signal peak. For every processor except the detector averager, each interval contained 20 statistically

independent noise samples. The two intervals were separated by a time gap centered on the signal peak. The width of this gap was ten times the pulse resolution time of the processor containing the signal peak.

For the detector averager, the length of the time gap was equal to two pulse lengths, the first time interval contained three independent samples, and the second time interval contained two independent samples. Larger intervals were not chosen since they would include the reverberation section of the output waveform. The reverberation noise level was considerably higher than the noise level in the waveform surrounding the signal peak.

c. Clutter Probability

In the manner described above, three sets of output values of peak minus mean over sigma were obtained, two sets from the generated data and one set from the recorded sea data. These values were then converted to individual sample clutter probabilities by the method described in Section IV. Graphs of number of signals detected vs clutter probability were then prepared. Such a graph for the SPC with three parallel channels appears in Figure 5. This particular graph was obtained from the set of ninety 175 c/s simulated echoes. In these graphs, a clutter probability is selected and the number of signals in the set detectable at that clutter probability is plotted on the vertical axis. For example, in Figure 5 the point on the graph with abscissa 0.001 has ordinate 28. This means that 28 signals in this particular set of 90 exceeded that threshold which noise alone exceeds with probability 0.001. This is equivalent to the statement that 0.001 is the clutter probability at which 28/90 of the signals were detectable. The detection graphs for all of the processors are contained in the attached Appendix. From each of these graphs, the clutter probability at which 50% of the signals were detectable was obtained. This clutter probability was multiplied by the output bandwidth to obtain the output clutter

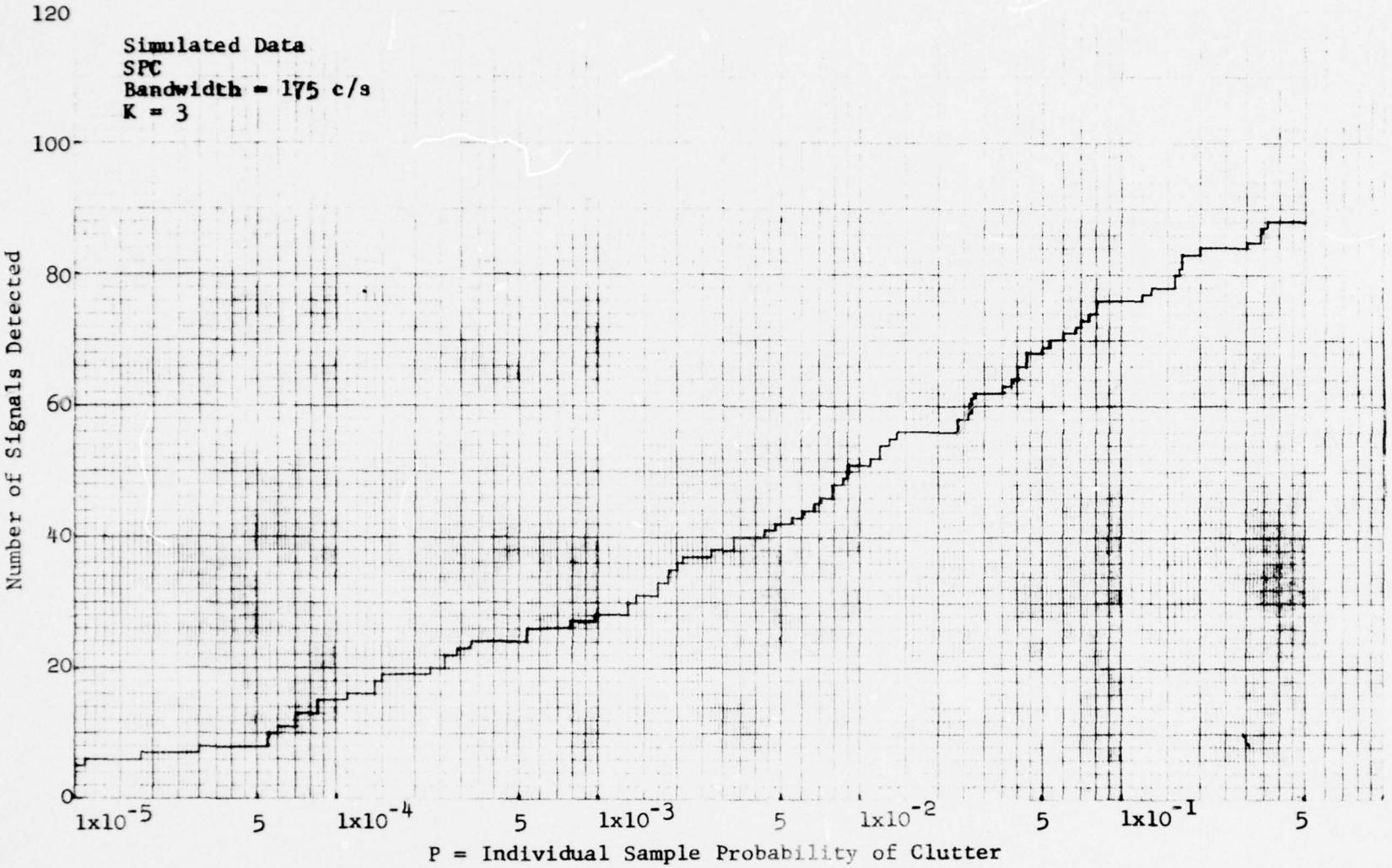

Figure 5 DETECTION STATISTICS: SPC

rate in clutter points per second. The corresponding clutter rates for 50% detection were obtained for each of the processors.

VI. RESULTS

The results obtained are shown in Figures 6, 7, and 8. Figure 6 contains the final graph for the 175 c/s simulated data and Figure 7 contains the final graph for the 350 c/s simulated data. Figure 8 contains the graph for the 200 c/s echoes recorded at sea.

In these graphs, the clutter rate at which 50% of the signals in the set were detectable is plotted as a function of K. The points plotted as "0" are for the SPC with K parallel channels and the points plotted as "x" are for the K-overaveraged linear correlator.

These detection performance graphs are read in the following manner: A set of data is chosen, such as the recorded sea echoes (Figure 8). Reading the horizontal axis at K = 3, it is seen that the 3-overaveraged linear correlator detected 50% of the 17 echoes at a clutter rate of 0.0025 whereas the SPC with 3-parallel channels detected 50% of the same echoes with a clutter rate of 0.14. The lowest point on the graph is the 2-overaveraged linear correlator and it is judged the superior processor of those considered for this particular set of signals.

These curves indicate that for these three particular sets of signals,

1. at least one of the techniques of signal recombination improved the detection performance of the linear correlator,
2. in two of the three cases (350 c/s simulated data and 220 c/s sea data), the 2-overaveraged linear correlator was judged the superior processor,

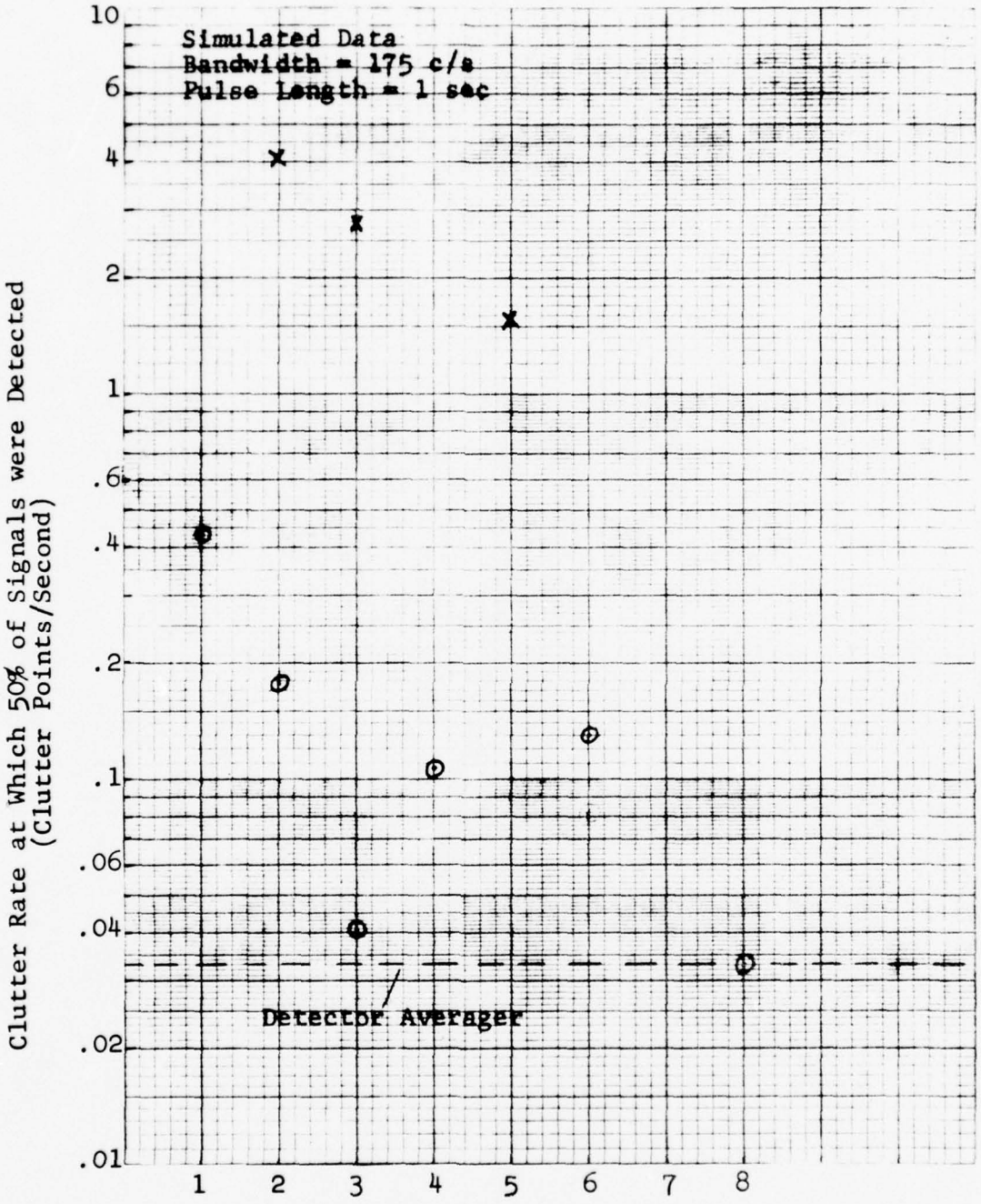

0 = Number of Correlators in Summed Partial Correlator

X = Number of Times Overaveraged

Figure 6 DETECTION PERFORMANCE CURVE
(175 c/s Simulated Echoes)

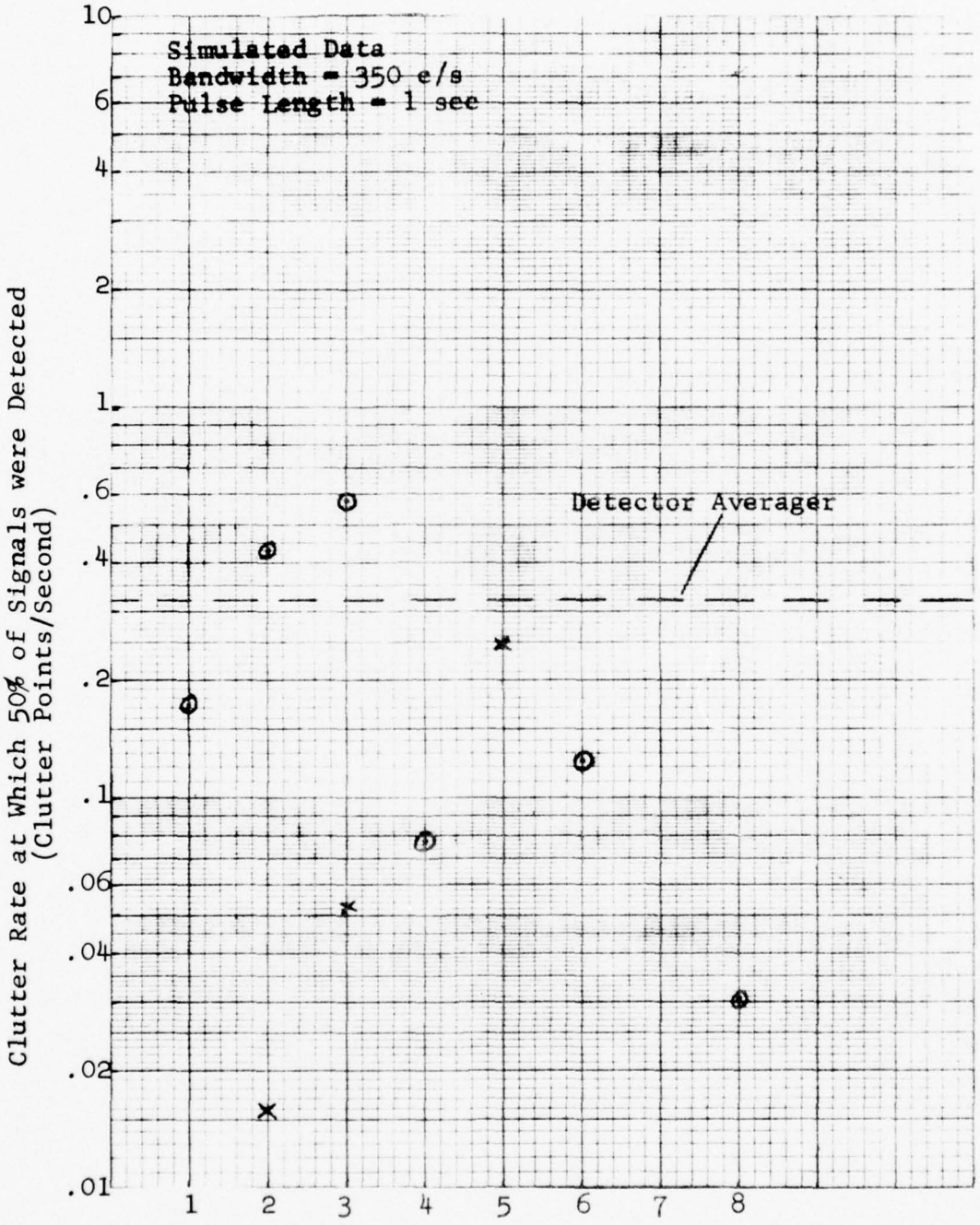

Θ = Number of Correlators in Summed Partial Correlator

X = Number of Times Overaveraged

Figure 7 DETECTION PERFORMANCE CURVE
(350 c/s Simulated Echoes)

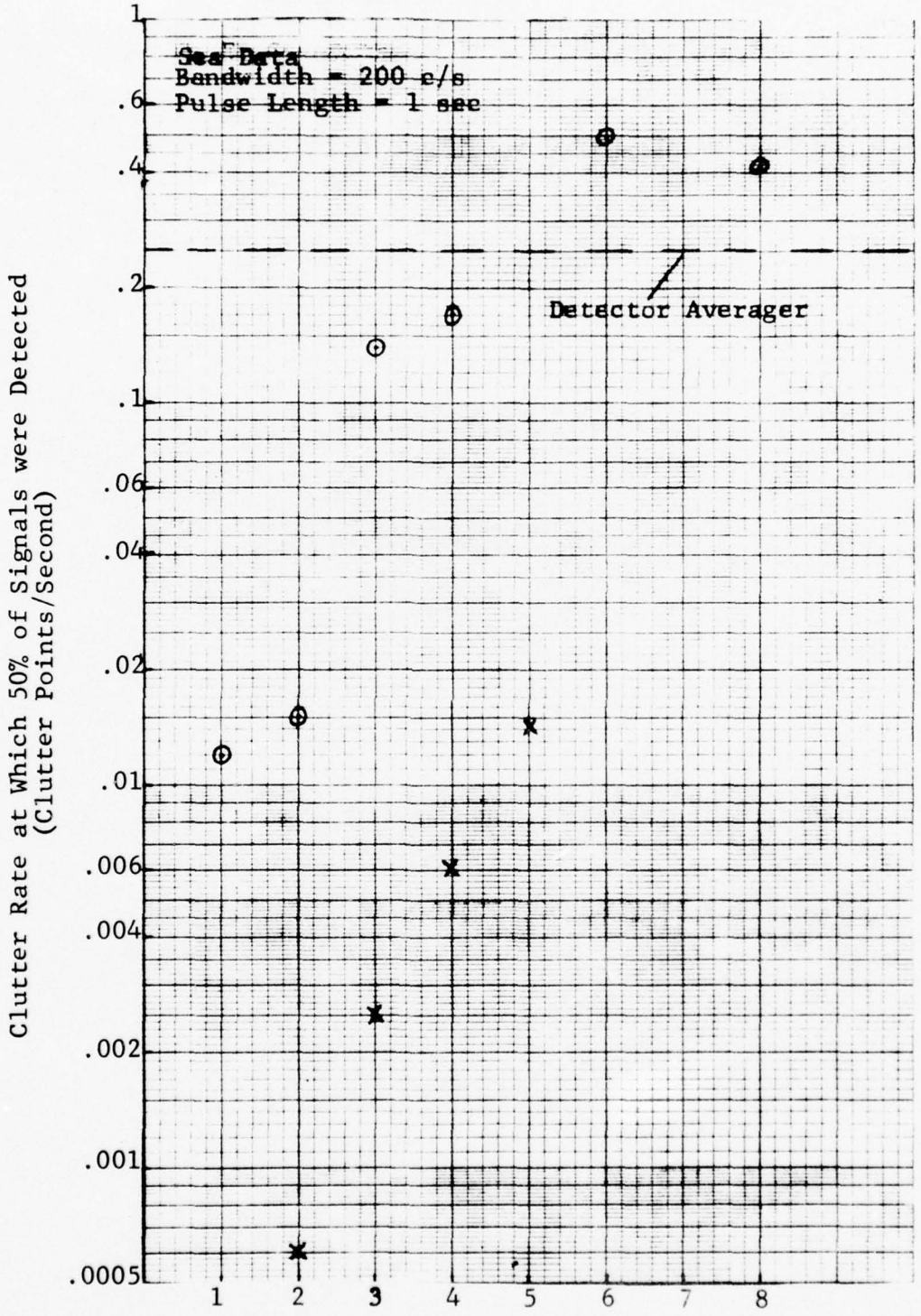

0 = Number of Correlators in Summed Partial Correlator

X = Number of Times Overaveraged

Figure 8 DETECTION PERFORMANCE CURVE
(200 c/s Echoes Recorded at Sea)

3. in the one case where the detector averager was judged superior (the 175 c/s simulated data), the SPC technique of signal recombination very nearly matched the detector for K = 3 and K = 8.

4. in all three graphs, the detection performance curve for the SPC has negative slope at K = 8, suggesting that better SPC performance might be obtained with even larger values of K.

It cannot be too strongly emphasized that the recorded echo results were obtained from a small set of echo cycles and that the simulated results were obtained for the particular multiarrival pulse selected.

VII. RECOMMENDATIONS FOR FUTURE STUDY

In the analysis of energy-splitting and Doppler effects on echo structure in the AN/SQS-26 system, thousands of recorded echoes were considered. To date less than one hundred recorded echoes have been employed in the analysis of signal recombination. It is therefore recommended that a much larger sample of recorded sea data be analyzed for the effectiveness of signal recombination.

These data should include a wide variety of echoes so that the following areas concerning the effectiveness of the SPC and overaveraging techniques may be investigated.

a. The dependence of optimum K upon pulse length and bandwidth for a given environmental condition.

b. The dependence of optimum K for a given bandwidth and pulse length upon sonar-target-propagation path geometry.

c. The performance of the SPC with relatively large values of K (such as 10 and 15).

APPENDIX

This appendix contains the clutter probability curves obtained for each of the processors considered in this report. The processor and type of data associated with a particular curve may be identified by the label in the upper left-hand corner of each graph.

In these graphs, the number of signals detectable at a clutter probability P is plotted as a function of P.

The manner in which these curves were obtained is described in detail in Section 5, Part C of this report.

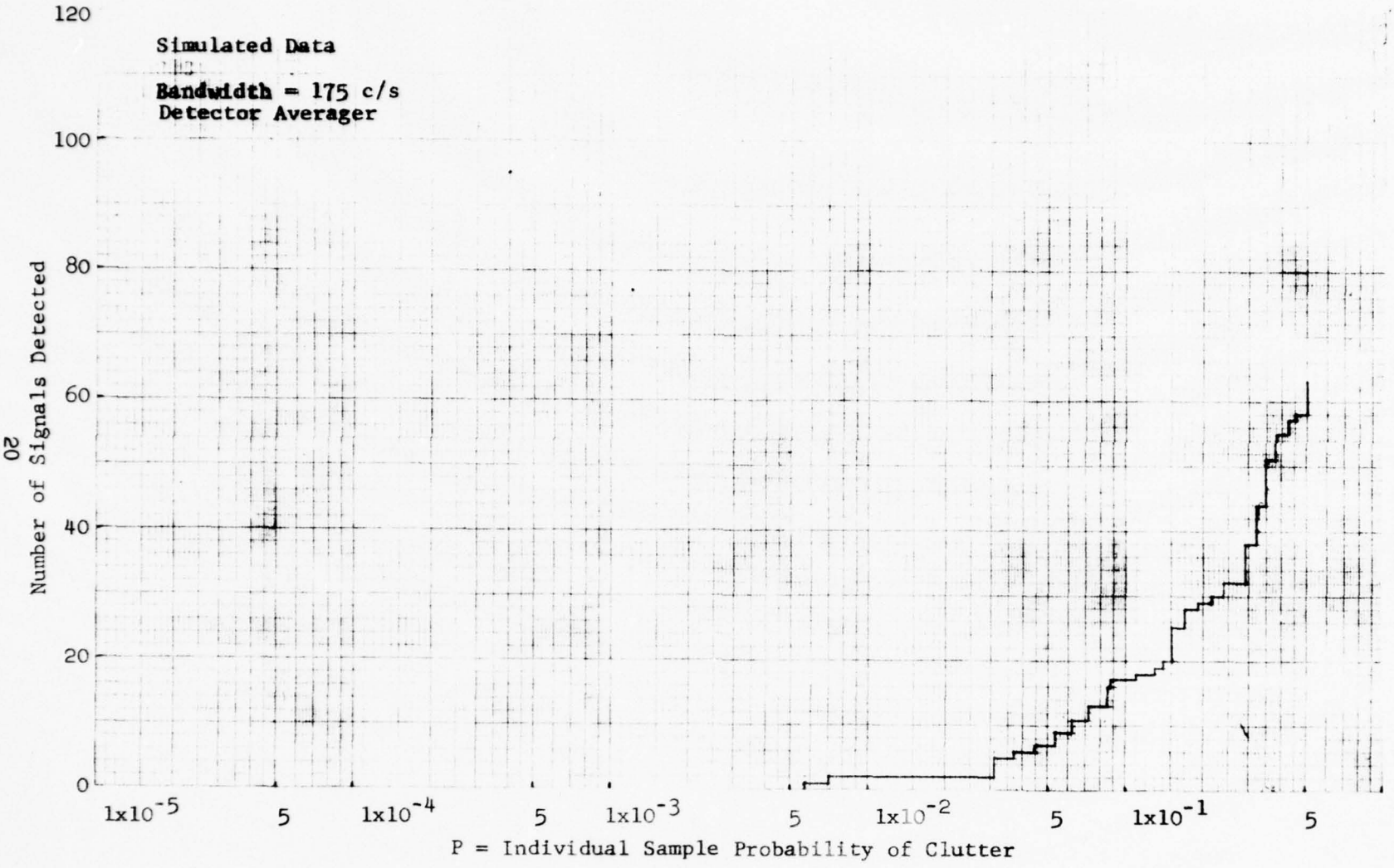

Figure 9 DETECTION STATISTICS: DETECTOR AVERAGER

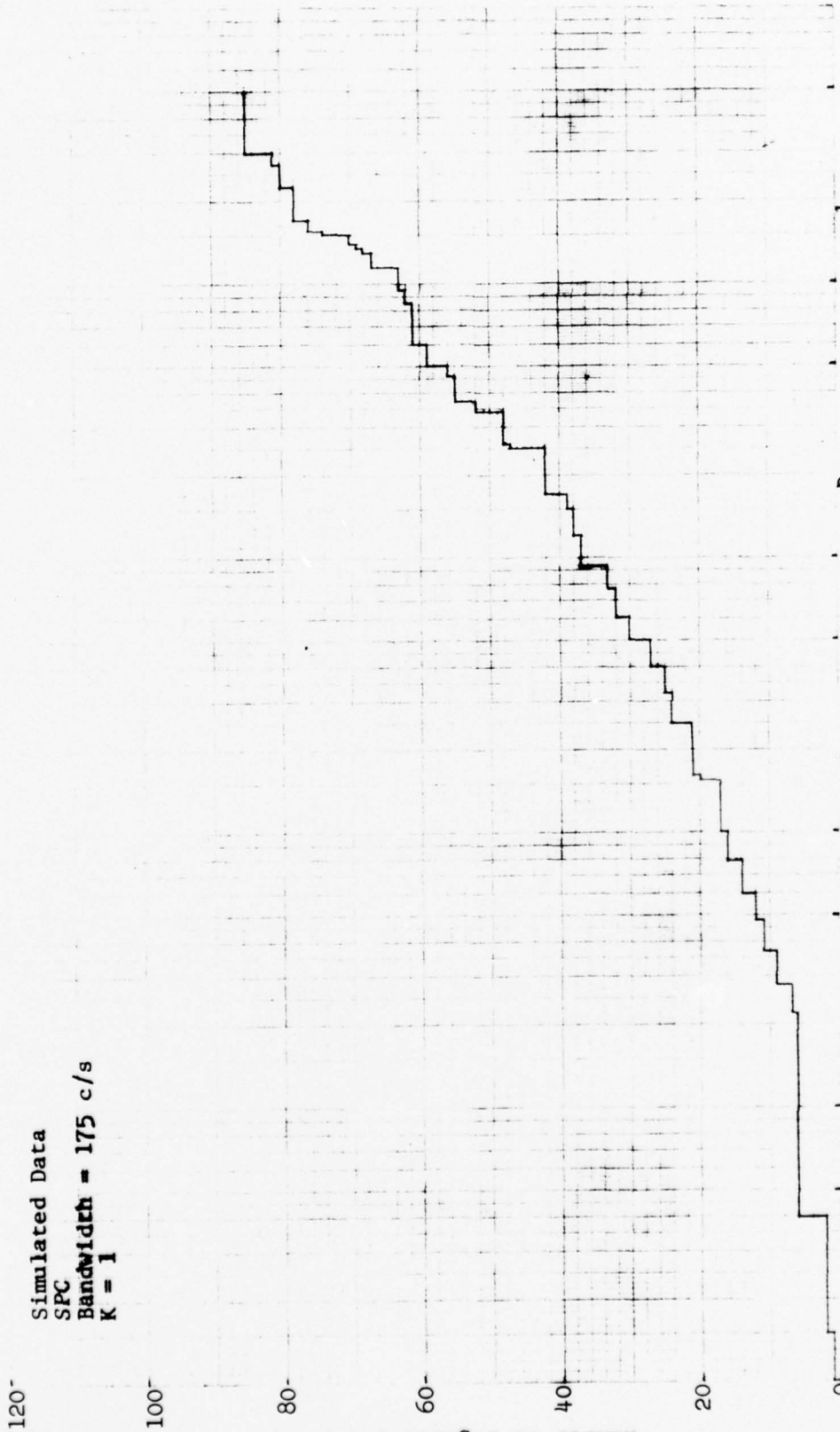

Figure 10 DETECTION STATISTICS: SPC

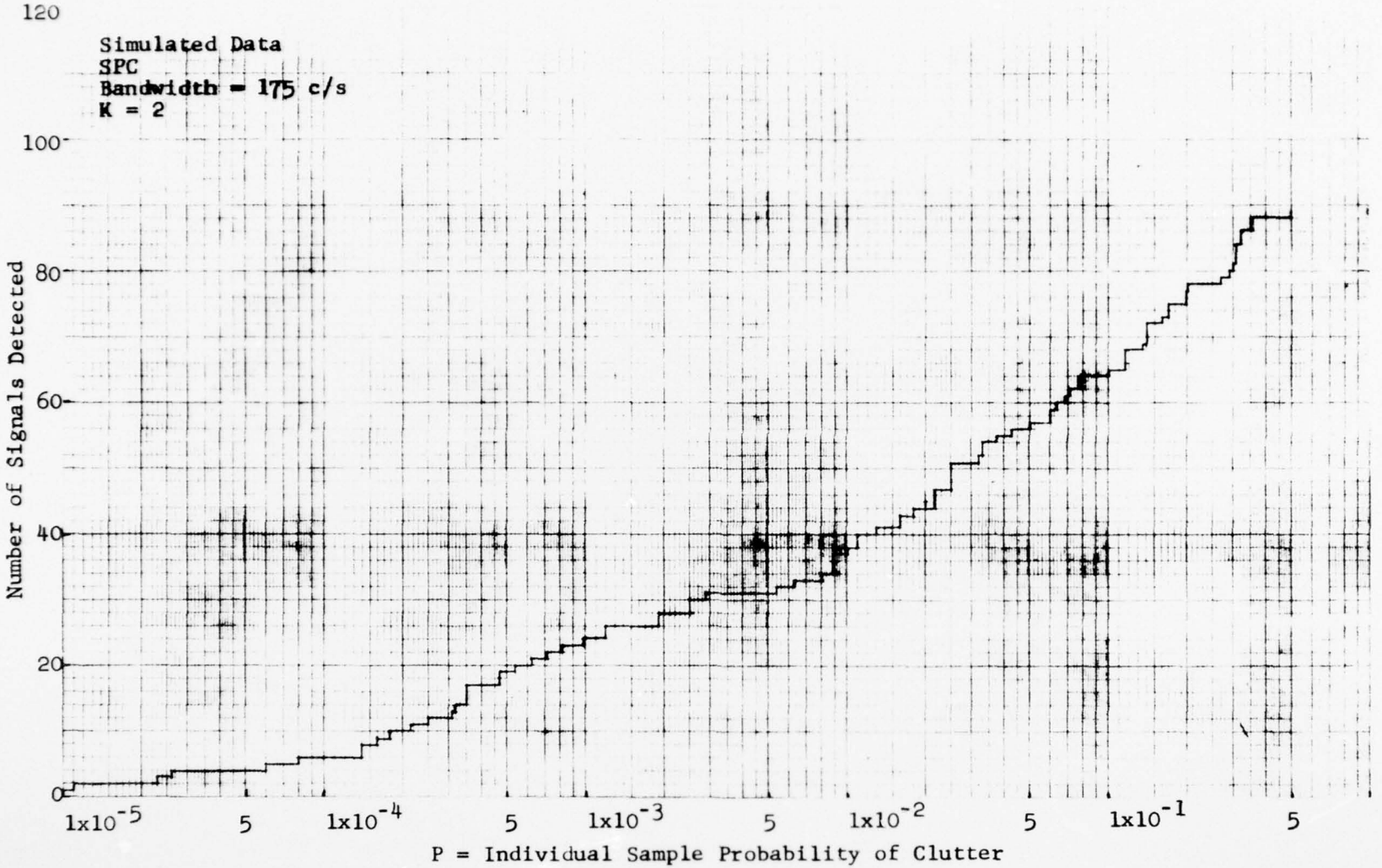

Figure 11 DETECTION STATISTICS: SPC

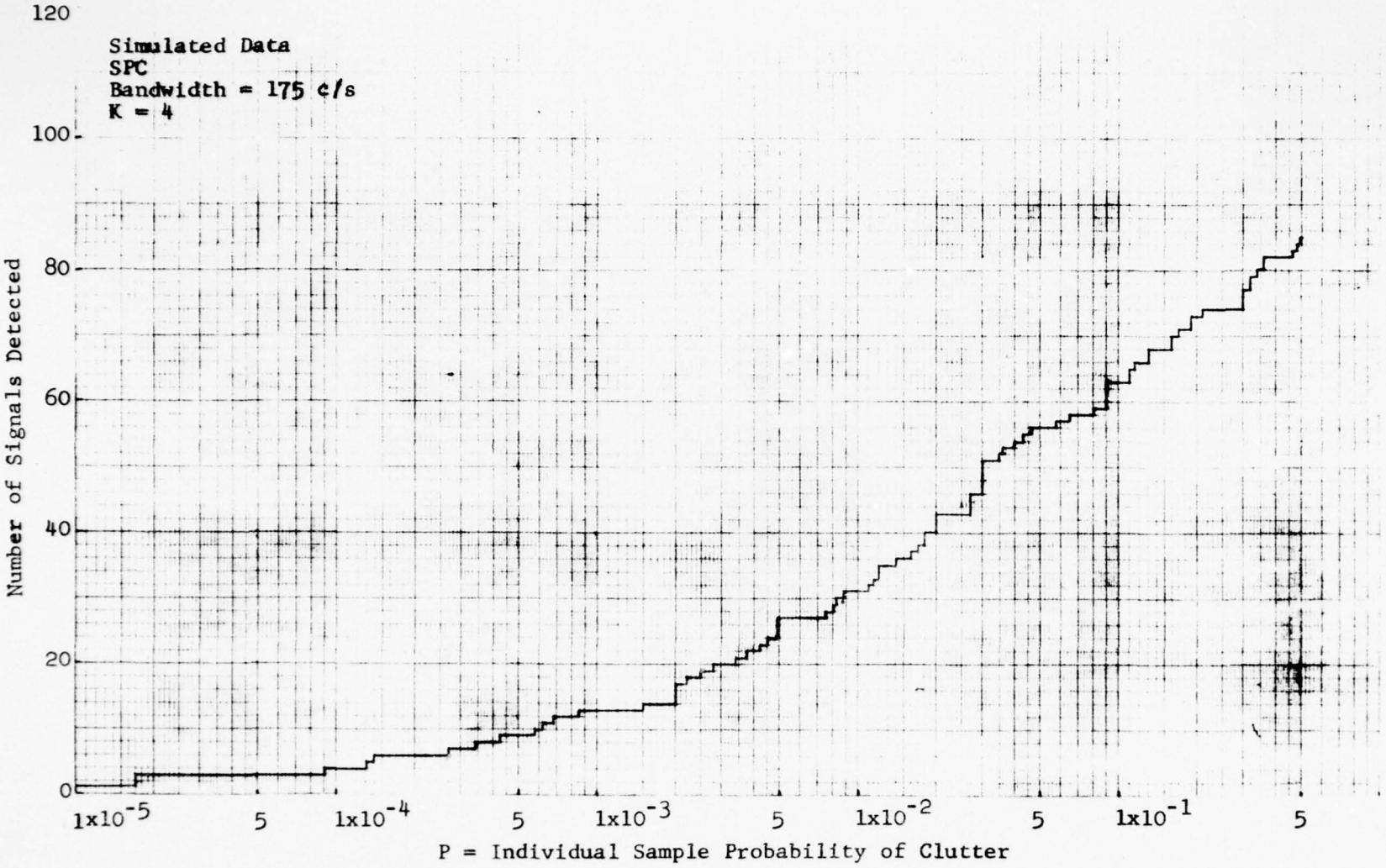

Figure 12 DETECTION STATISTICS: SPC

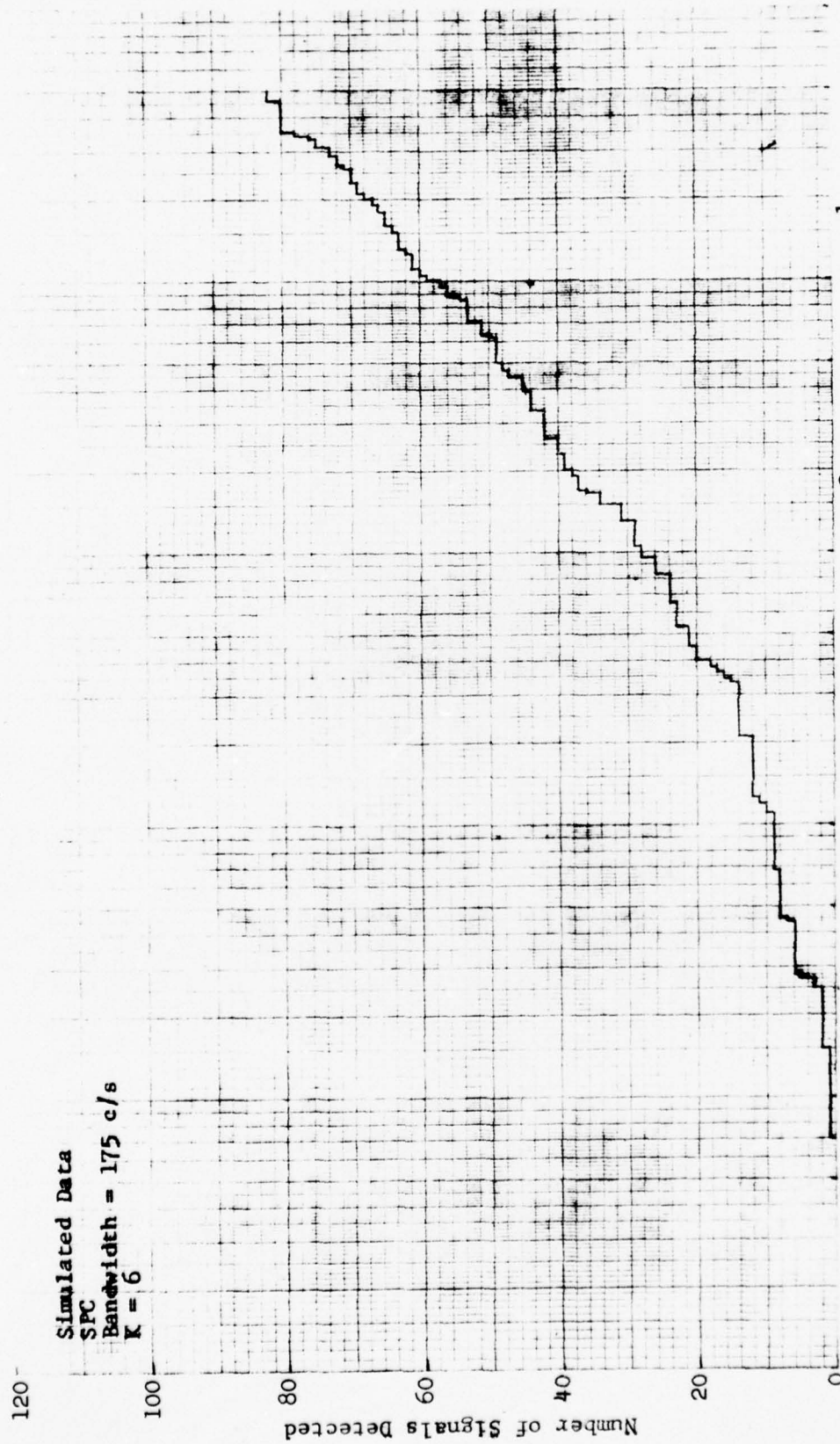

Figure 13 DETECTION STATISTICS: SPC

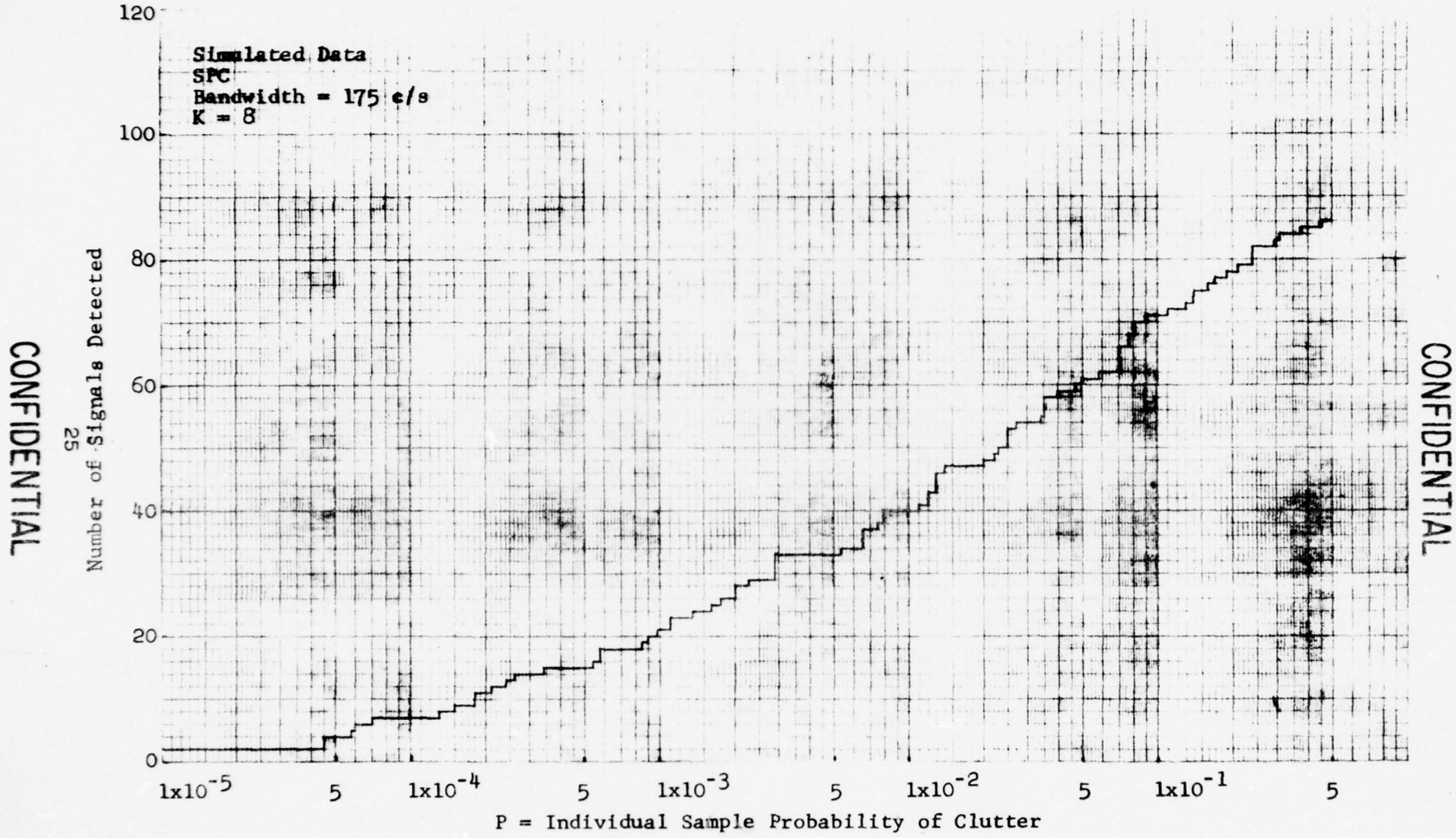

Figure 14 DETECTION STATISTICS: SPC

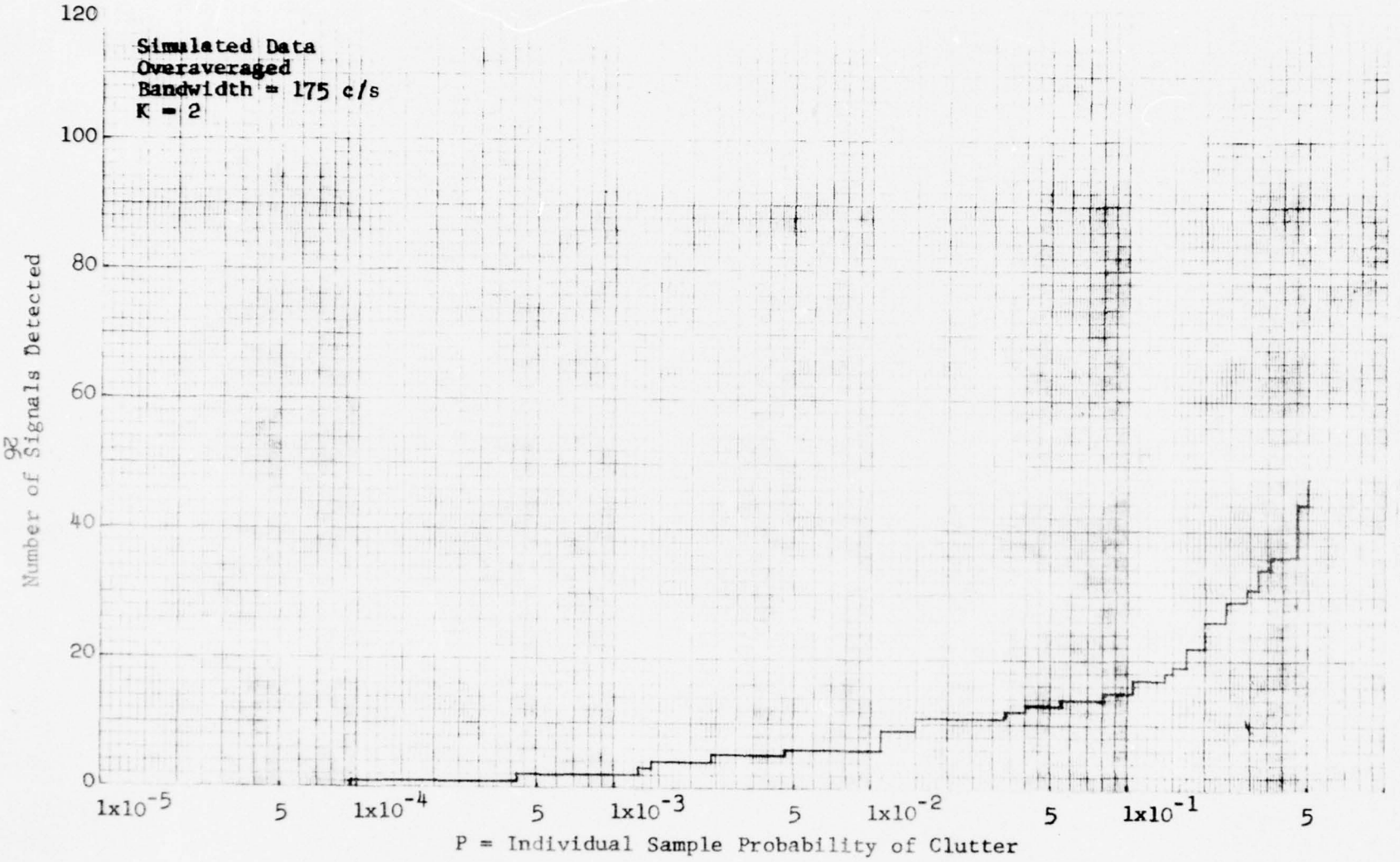

Figure 15 DETECTION STATISTICS: OVERAVERAGED LINEAR CORRELATOR

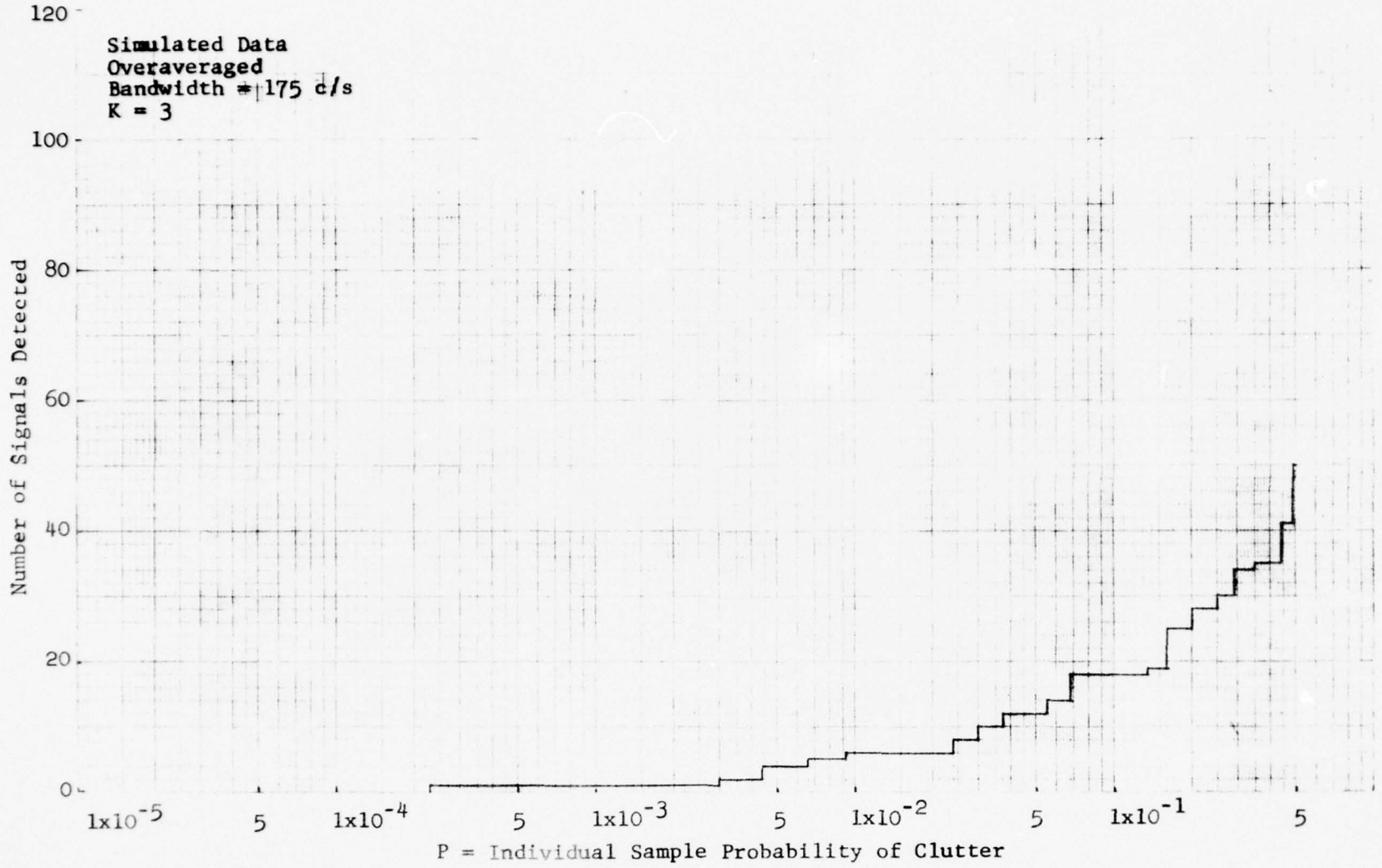

Figure 16 DETECTION STATISTICS: OVERAVERAGED LINEAR CORRELATOR

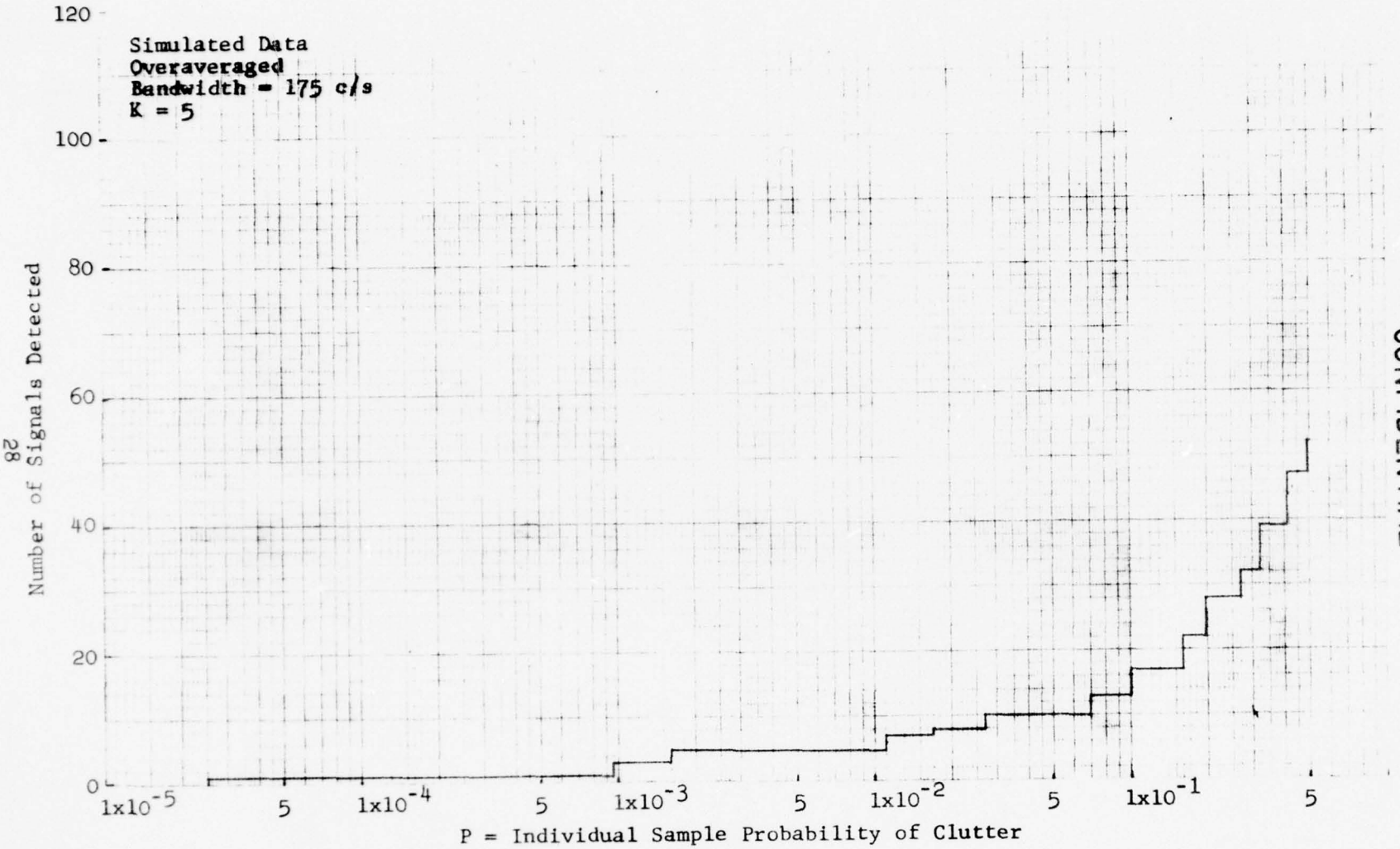

Figure 17 DETECTION STATISTICS: OVERAVERAGED LINEAR CORRELATOR

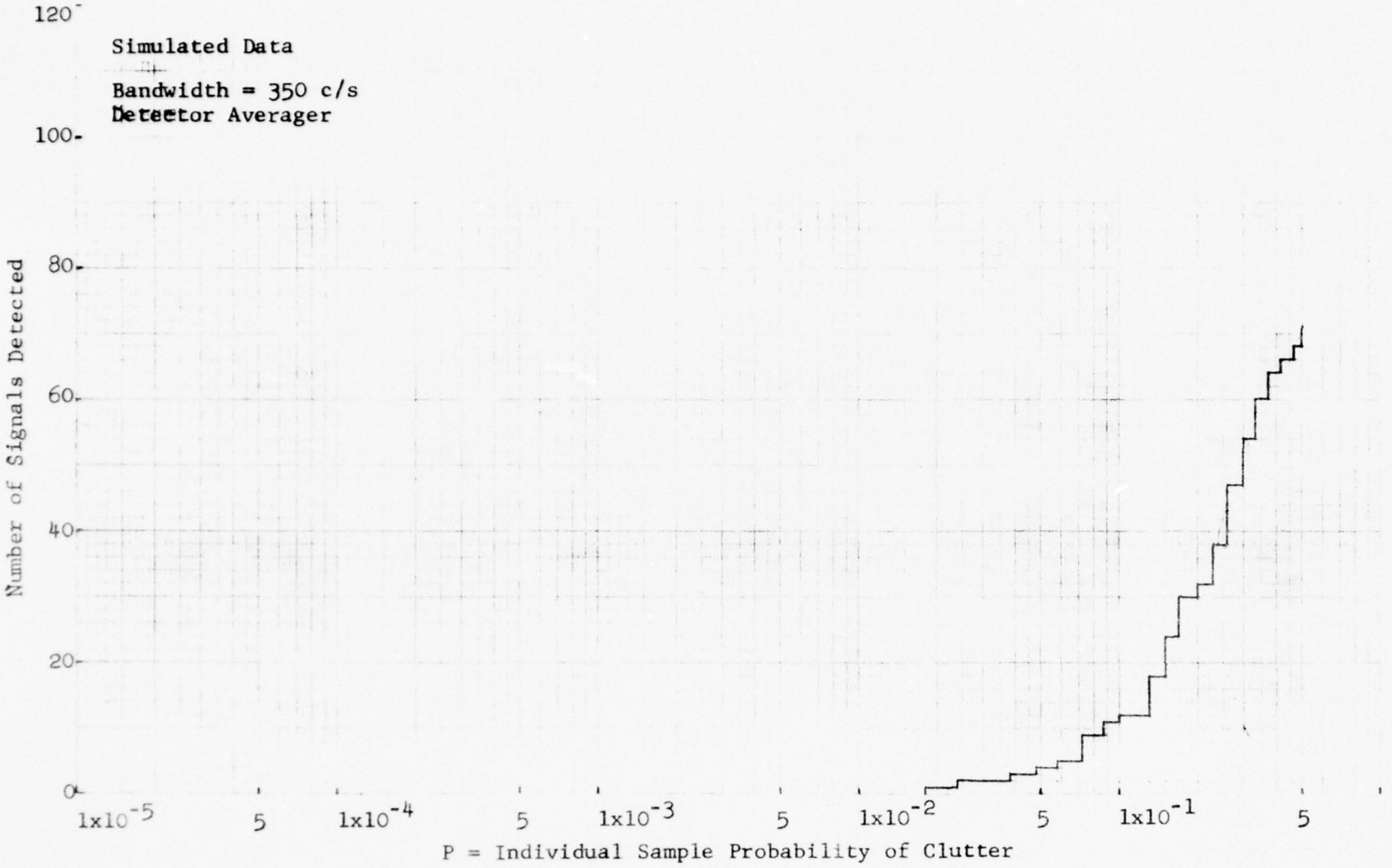

Figure 18 DETECTION STATISTICS: DETECTOR AVERAGER

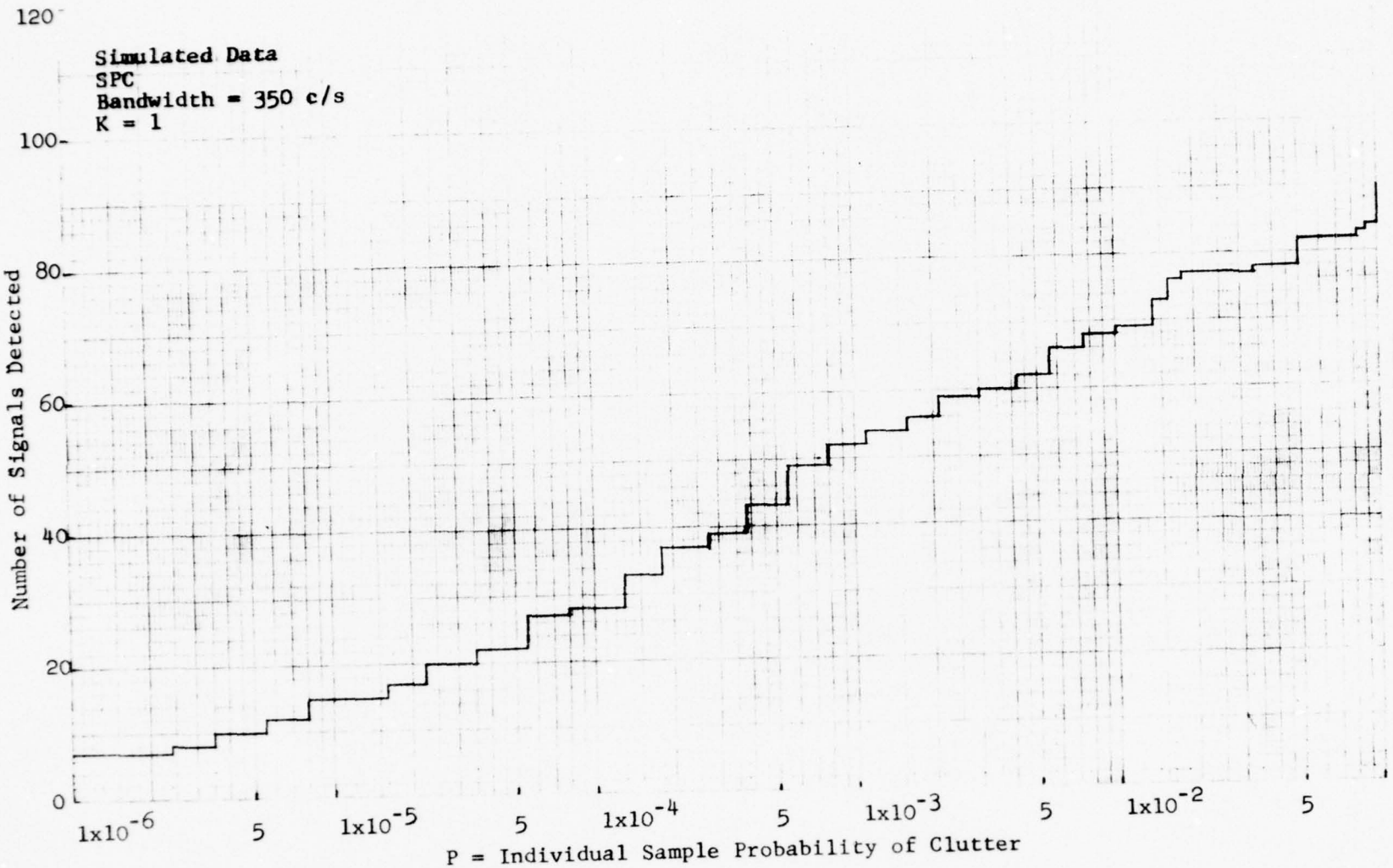

Figure 19 DETECTION STATISTICS: SPC

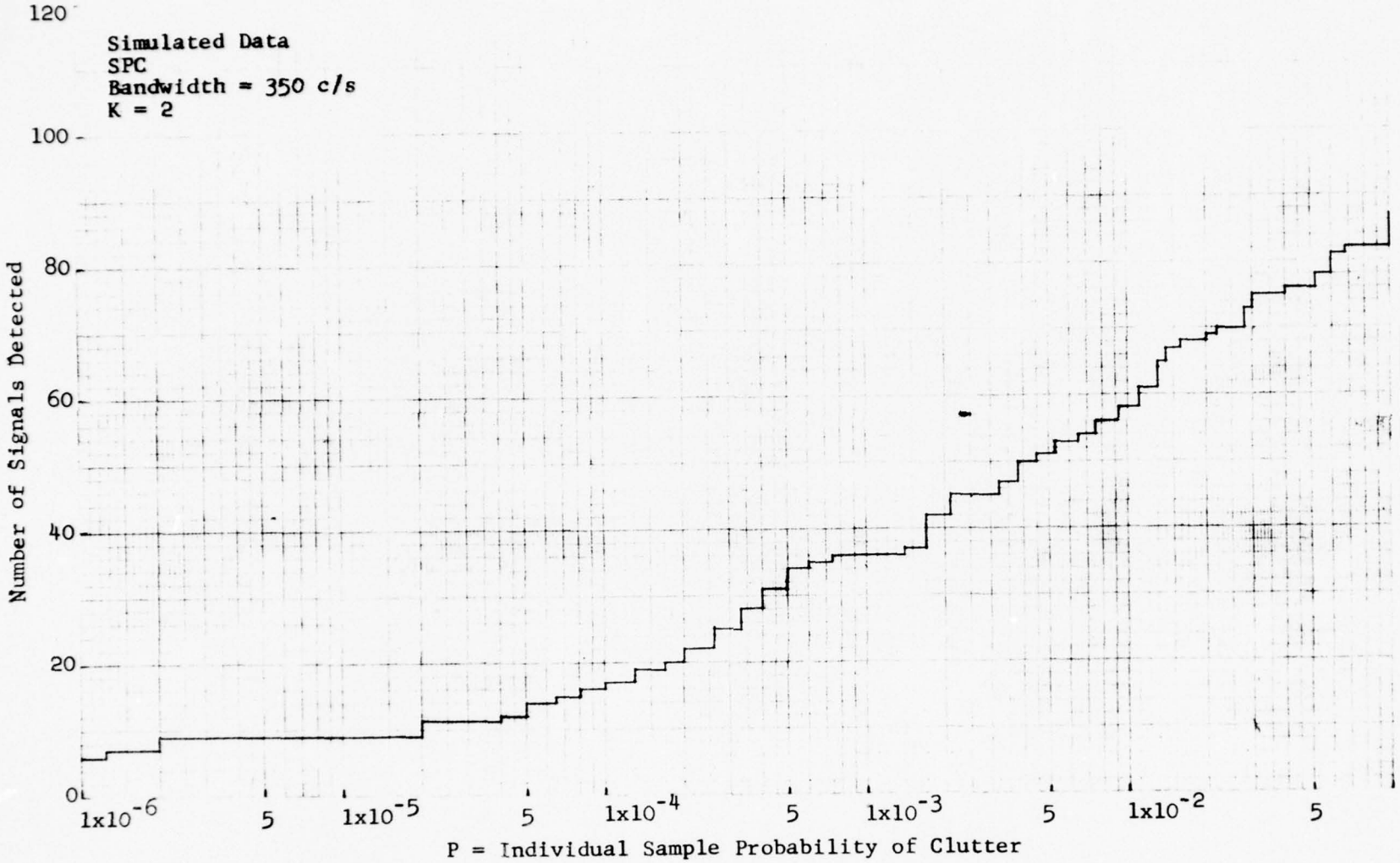

Figure 20 DETECTION STATISTICS: SPC

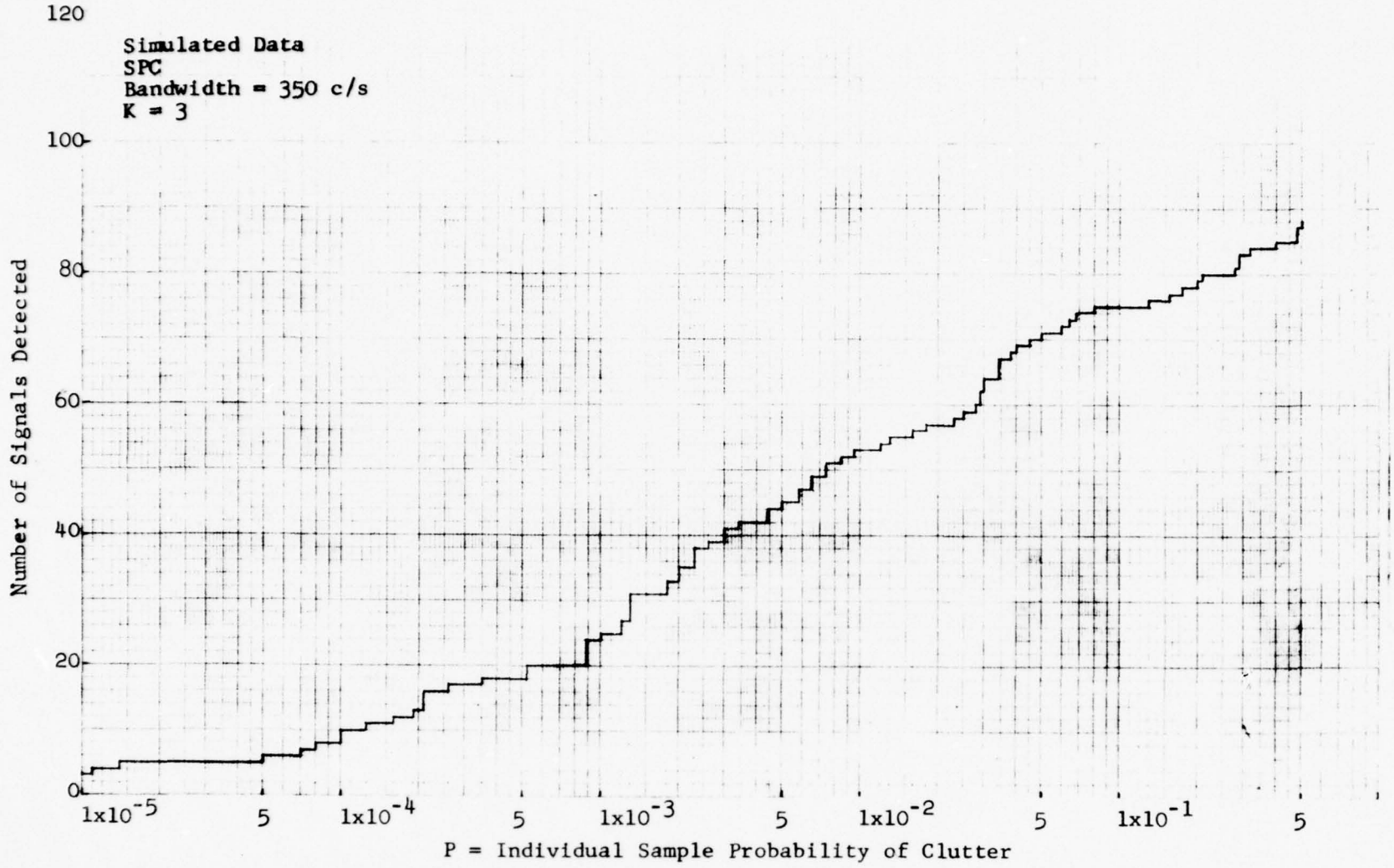

Figure 21 DETECTION STATISTICS: SPC

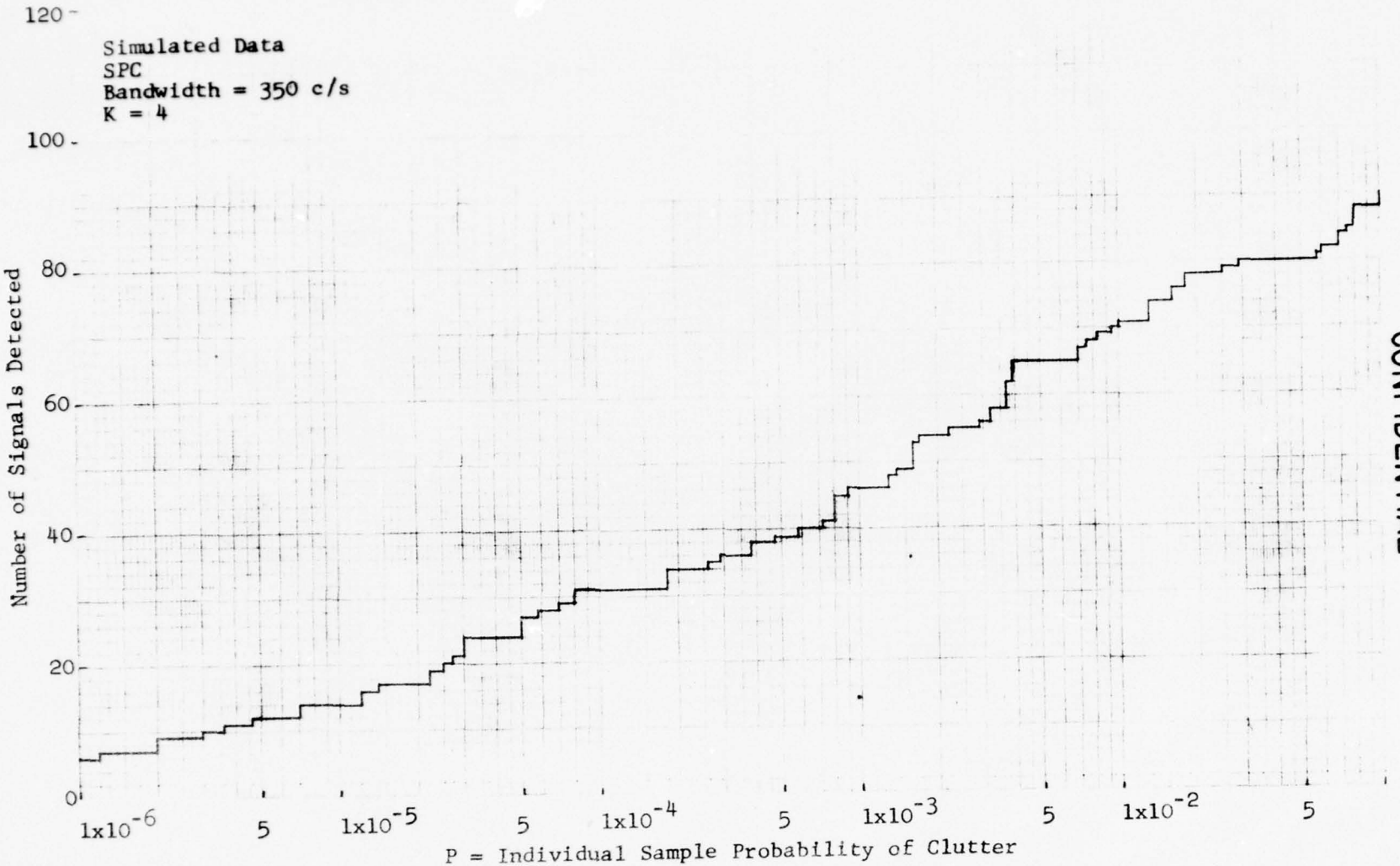

Figure 22 DETECTION STATISTICS: SPC

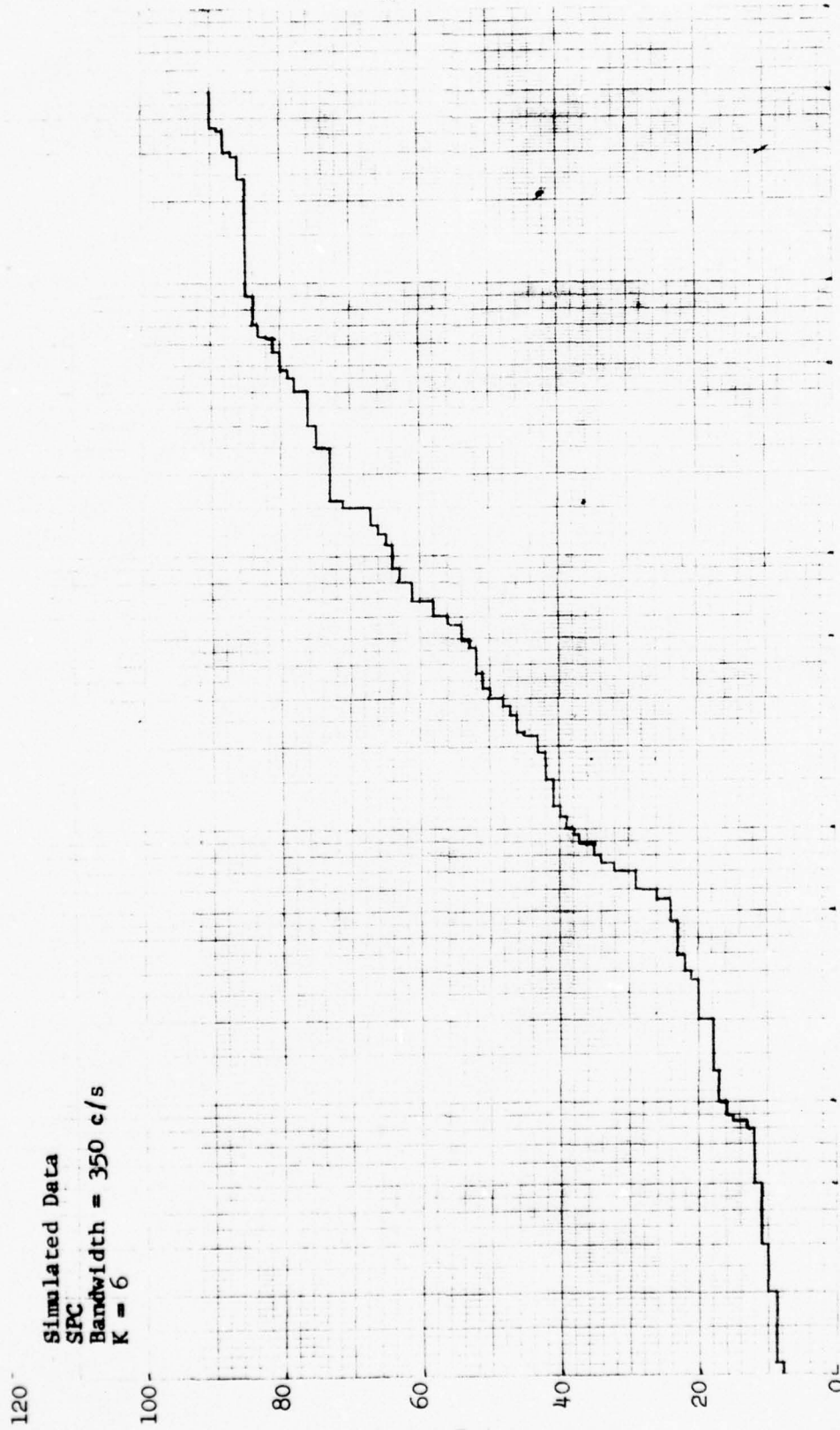

Figure 23 DETECTION STATISTICS: SPC

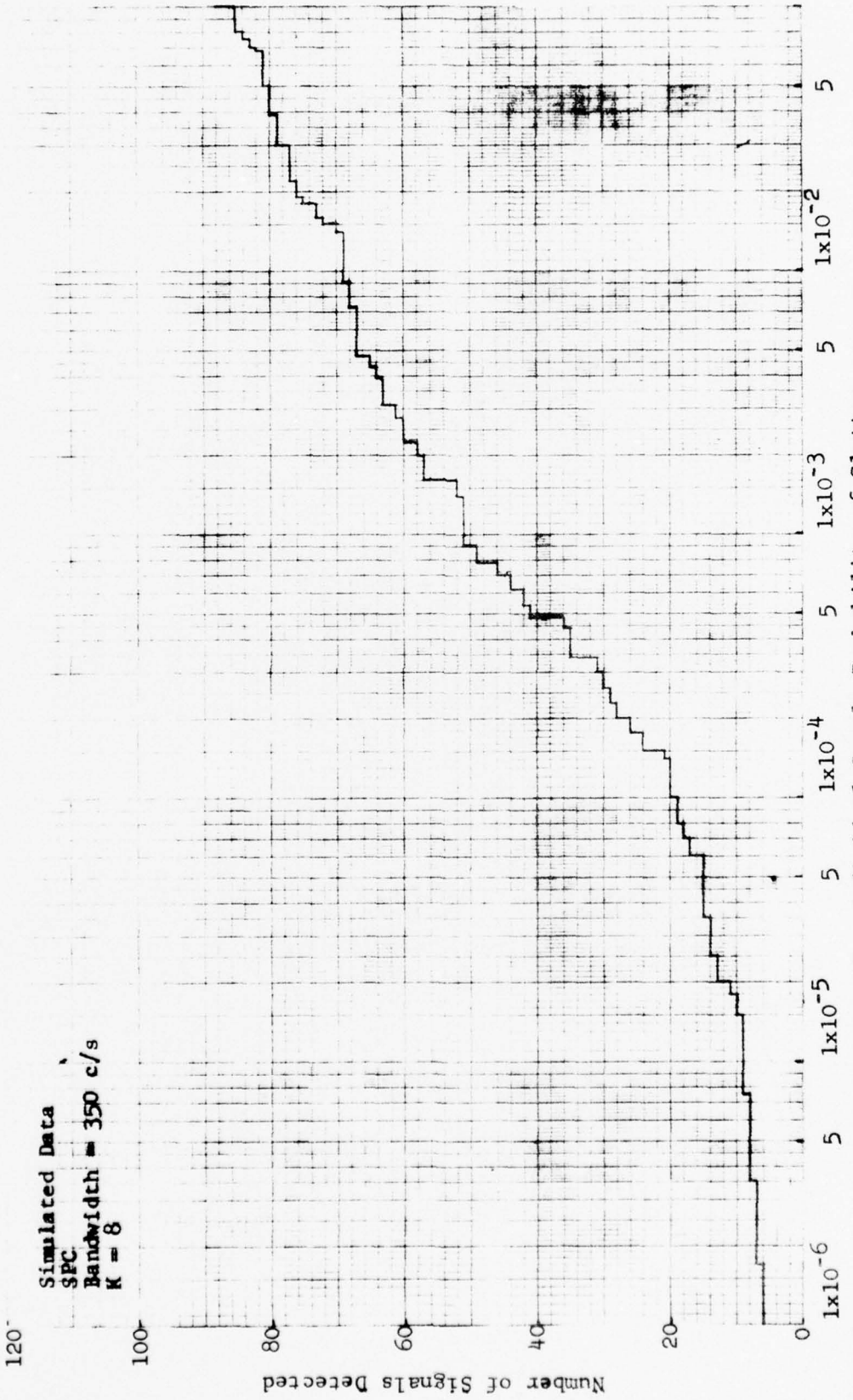

Figure 24 DETECTION STATISTICS: SPC

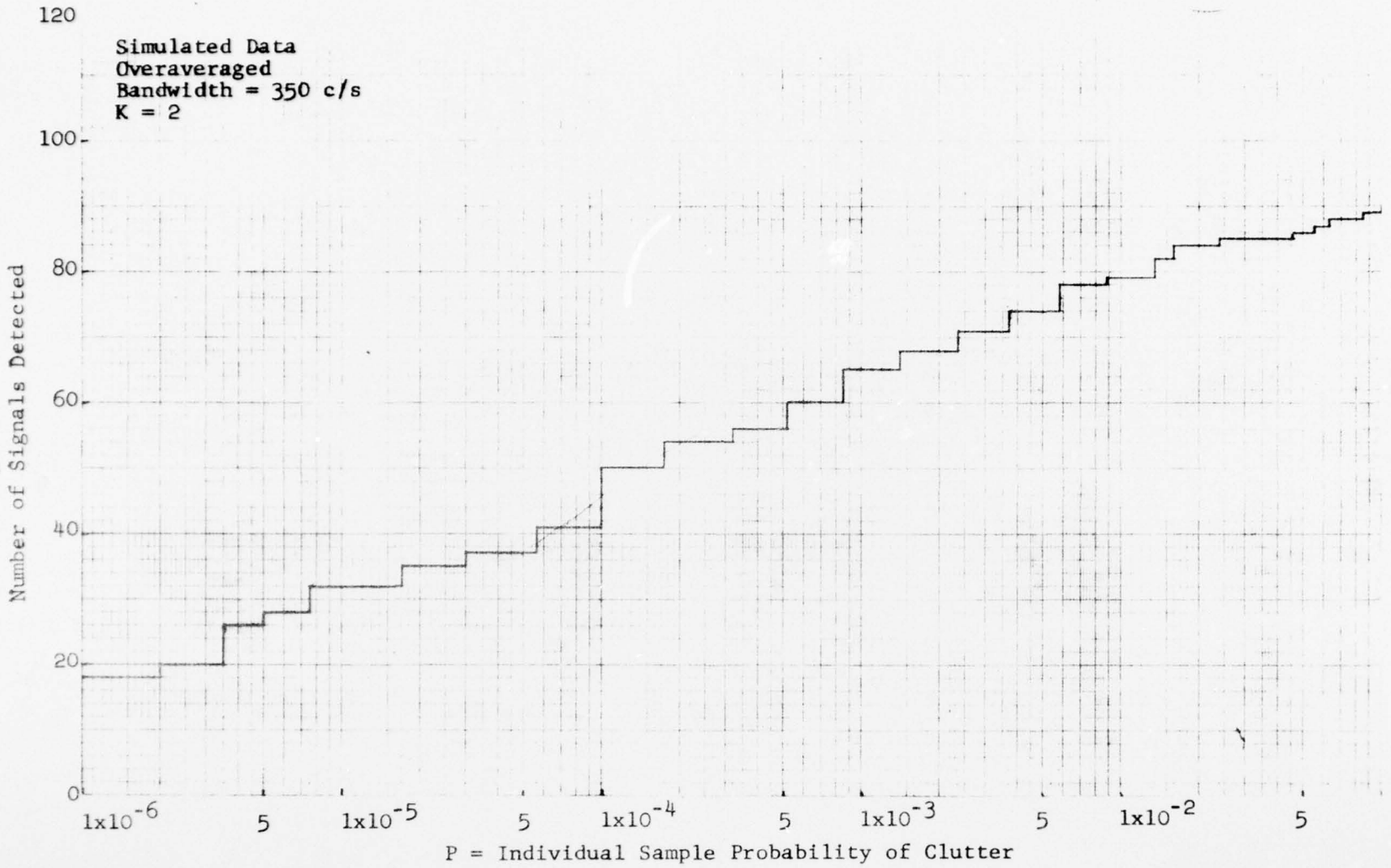

Figure 25 DETECTION STATISTICS: OVERAVERAGED LINEAR CORRELATOR

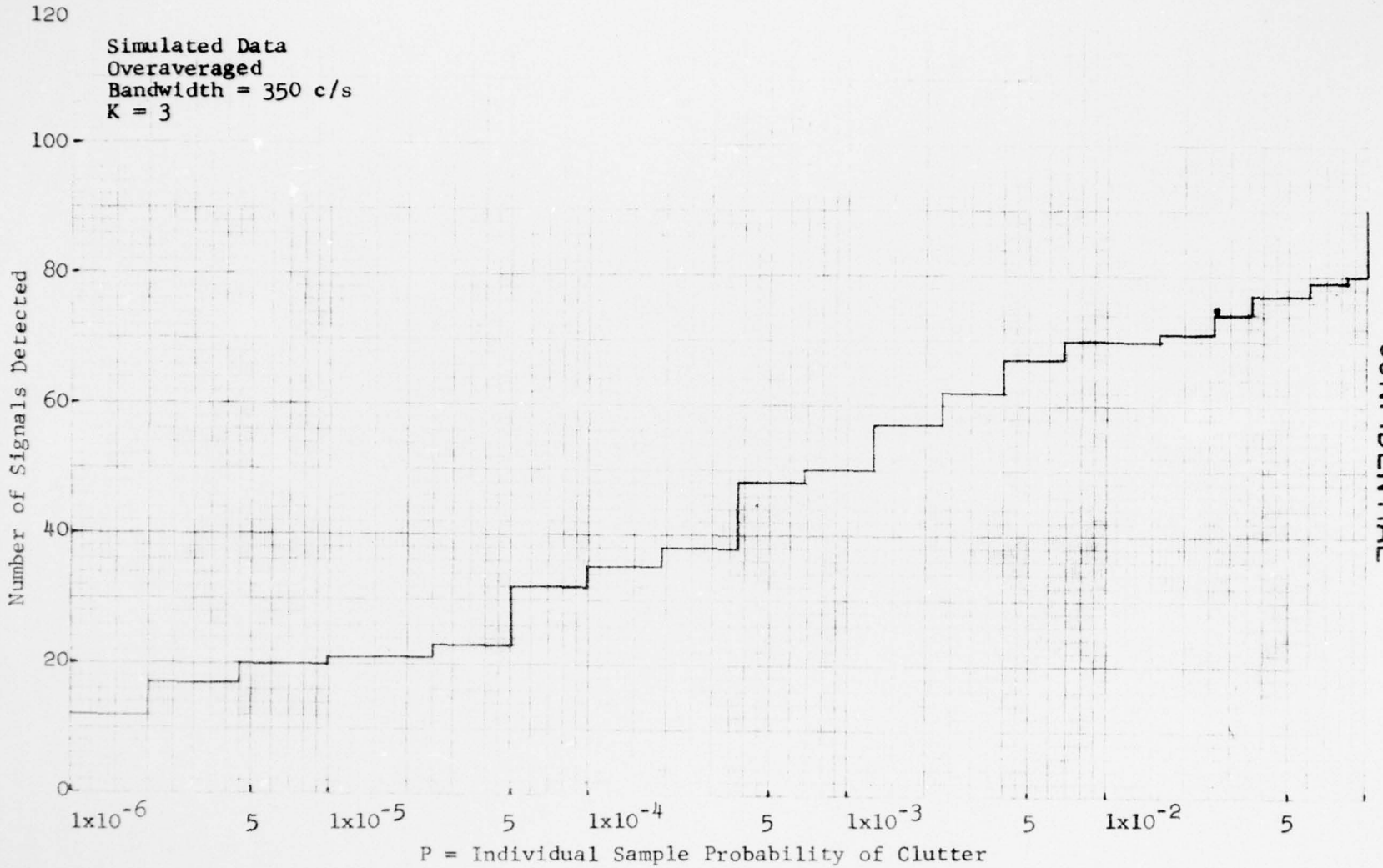

Figure 26 DETECTION STATISTICS: OVERAVERAGED LINEAR CORRELATOR

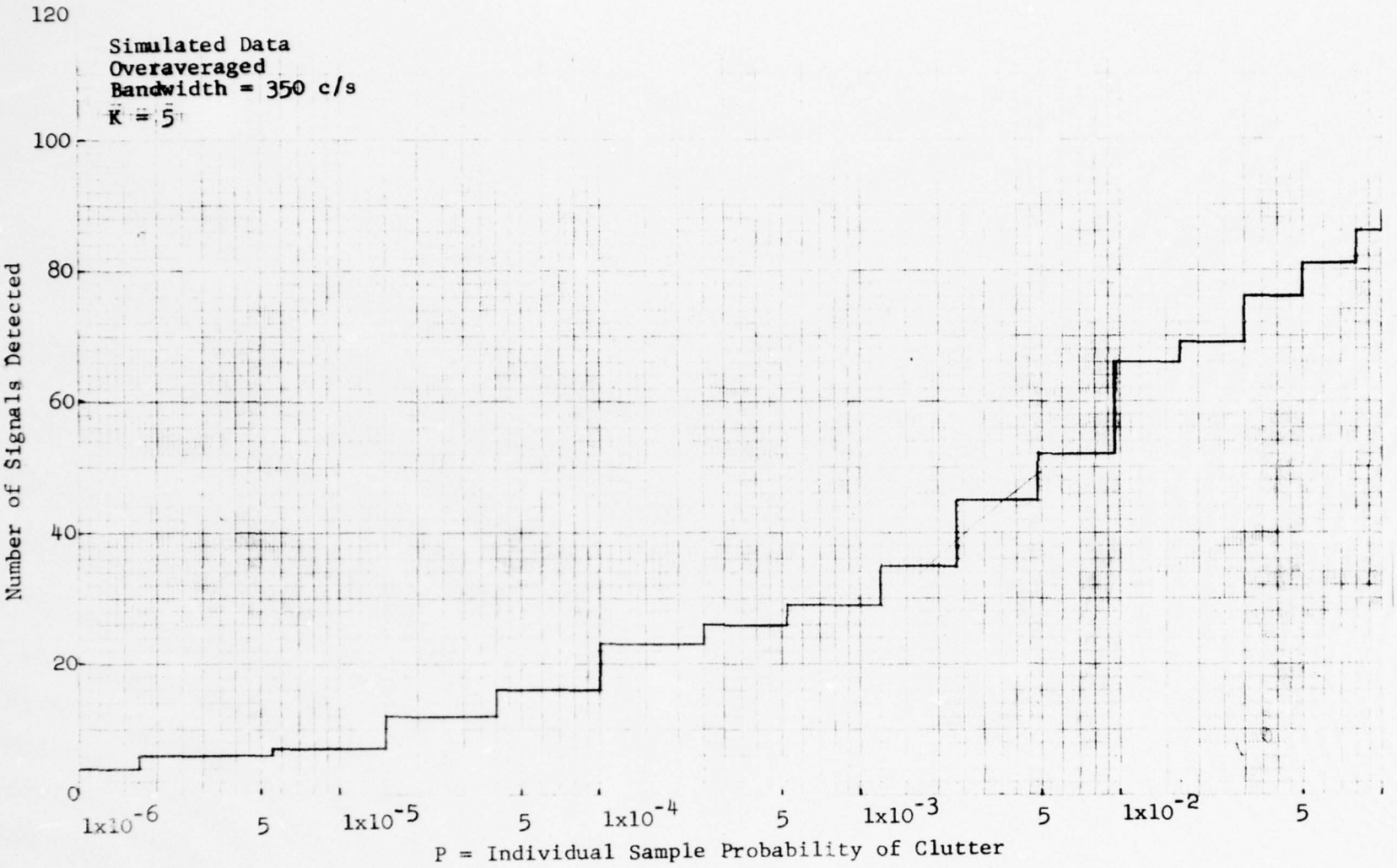

Figure 27 DETECTION STATISTICS: OVERAVERAGED LINEAR CORRELATOR

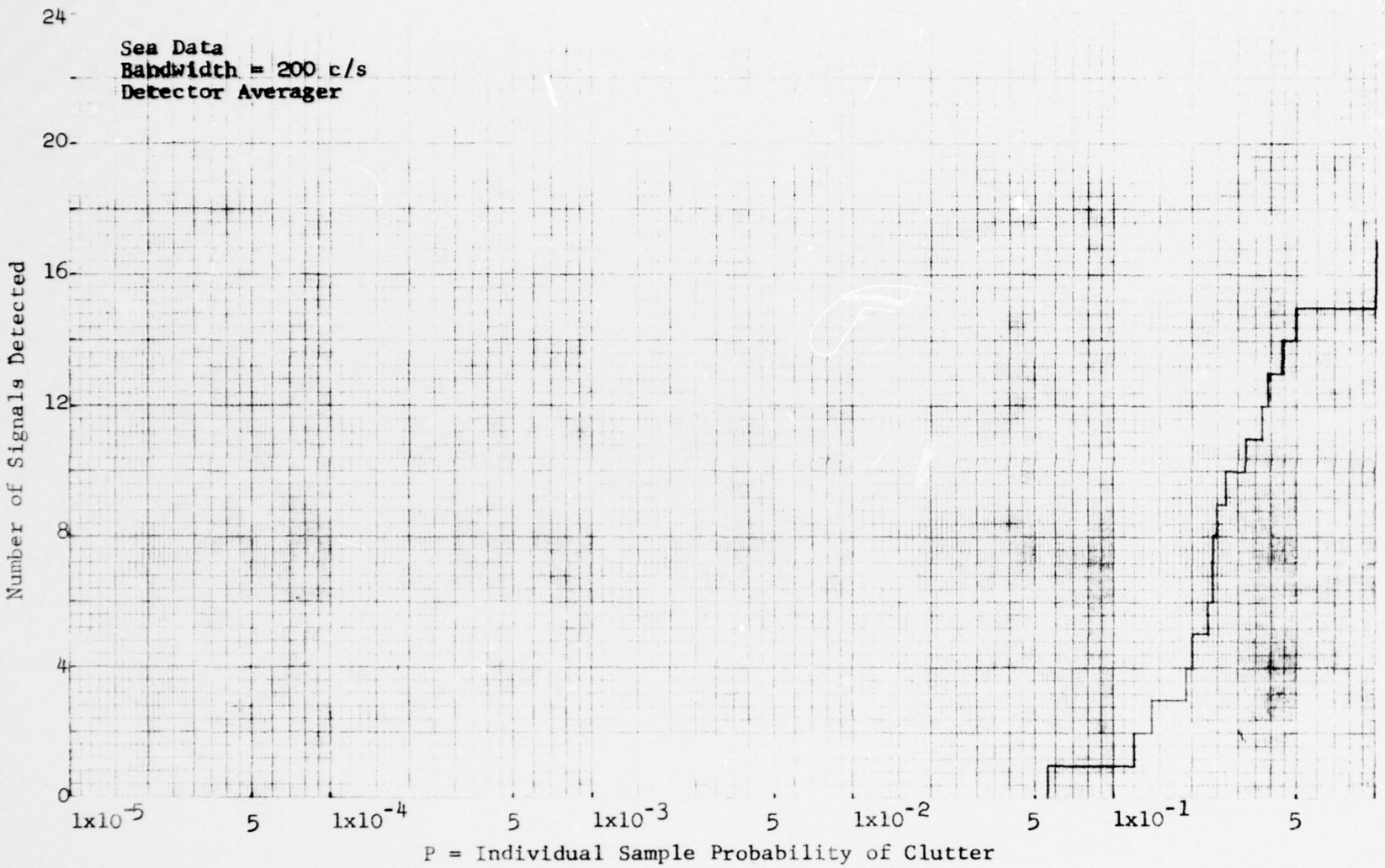

Figure 28 DETECTION STATISTICS: DETECTOR AVERAGER

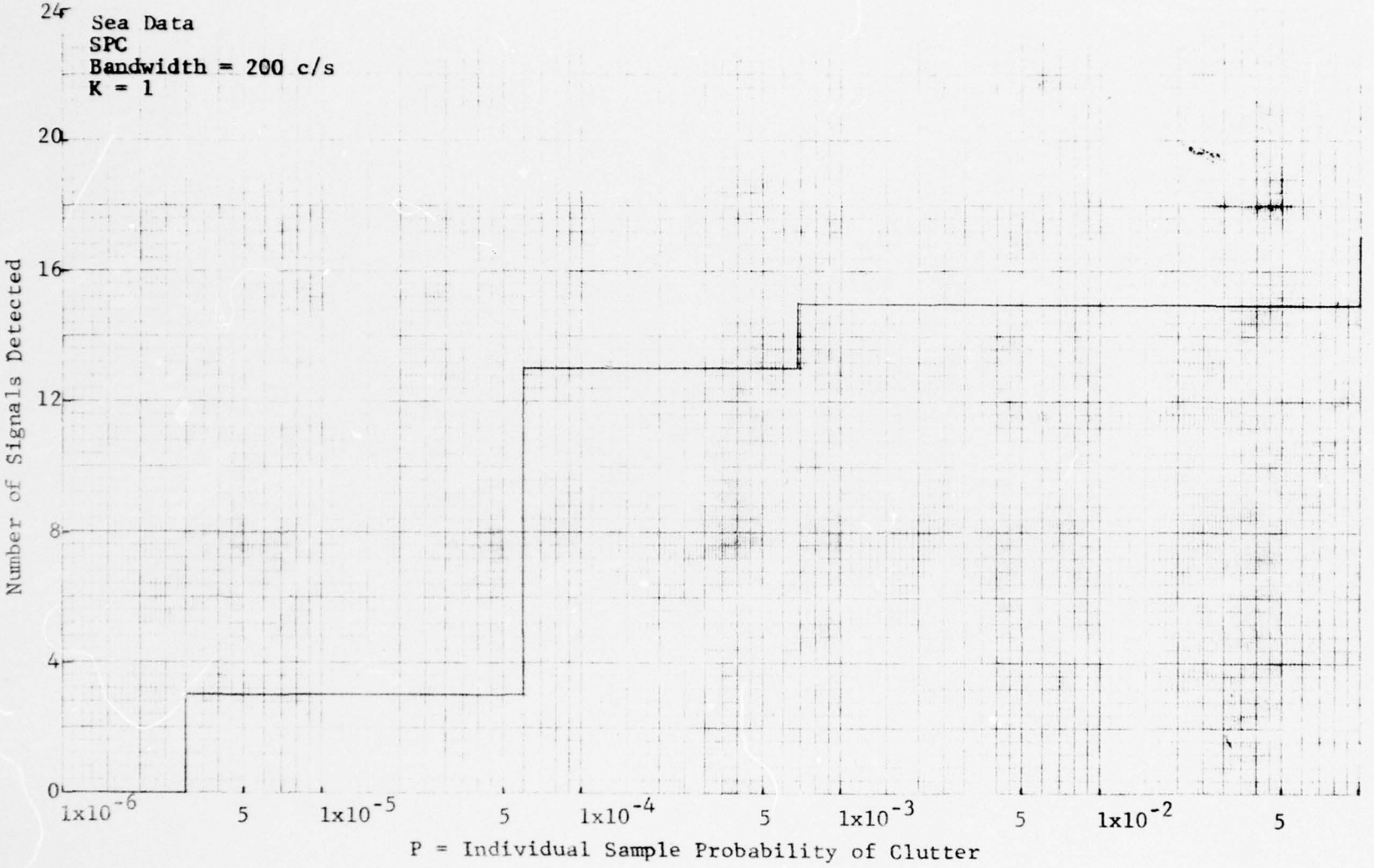

Figure 29 DETECTION STATISTICS: SPC

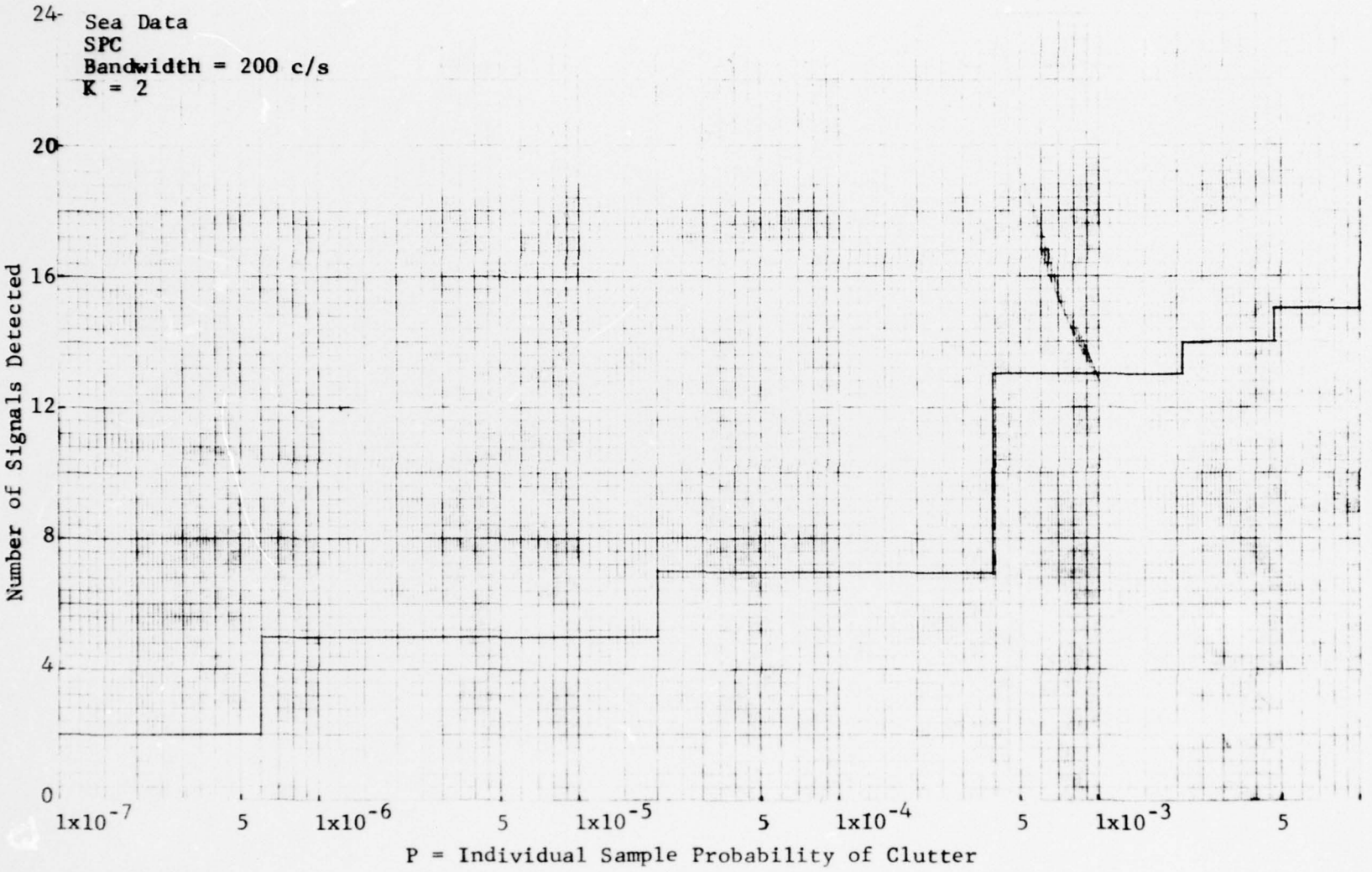

Figure 39 DETECTION STATISTICS: SPC

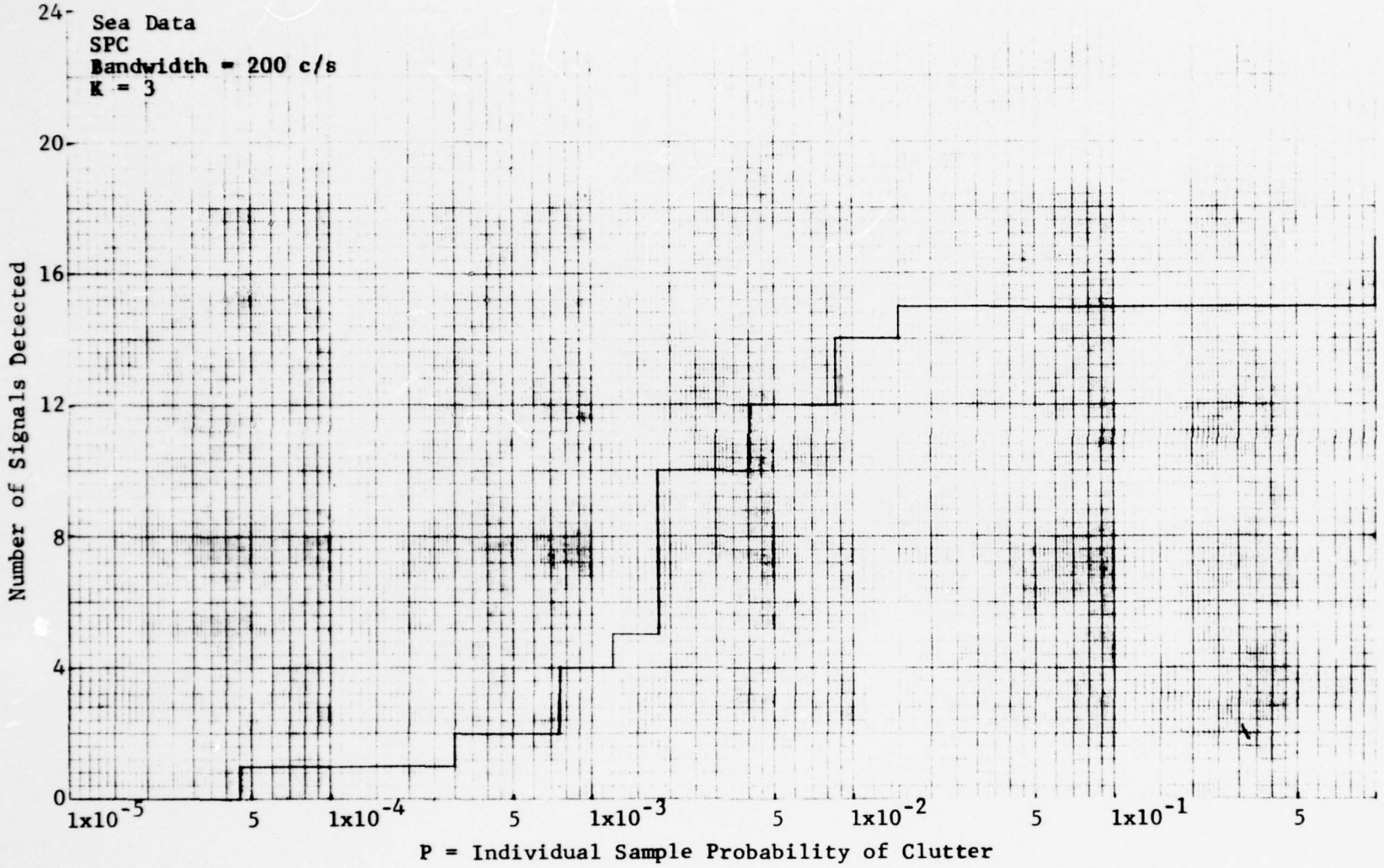

Figure 31 DETECTION STATISTICS: SPC

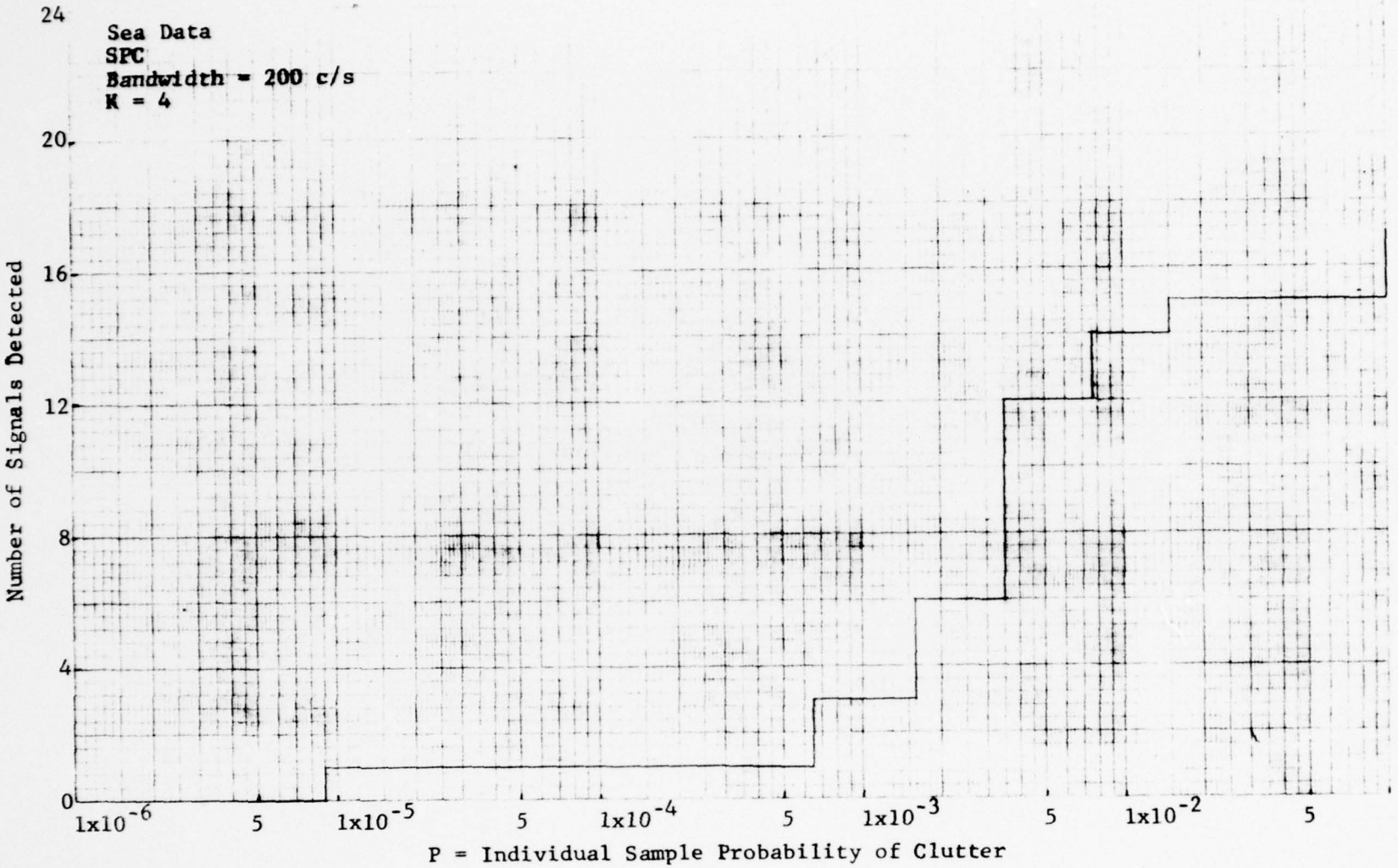

Figure 32 DETECTION STATISTICS: SPC

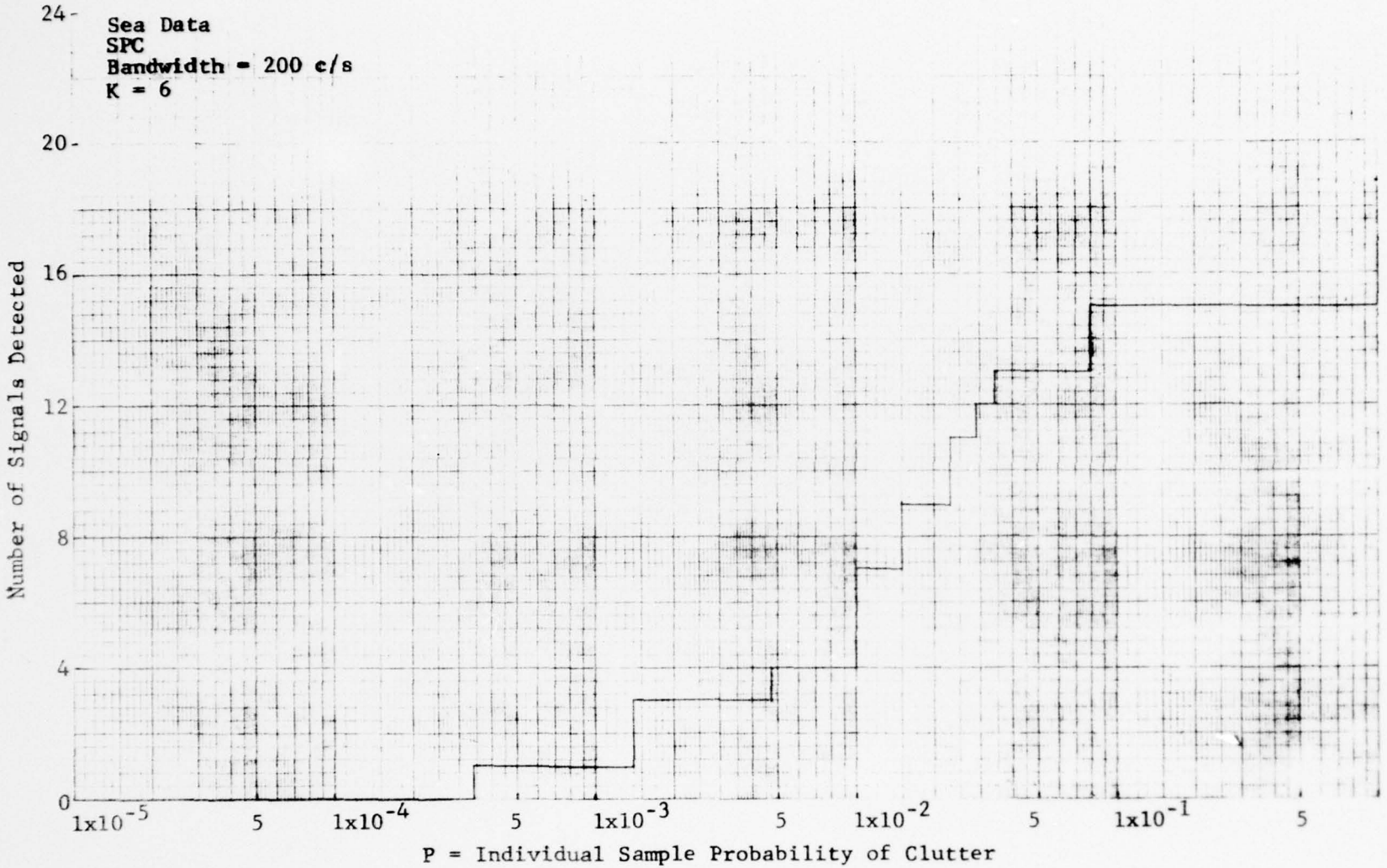

Figure 33 DETECTION STATISTICS: SPC

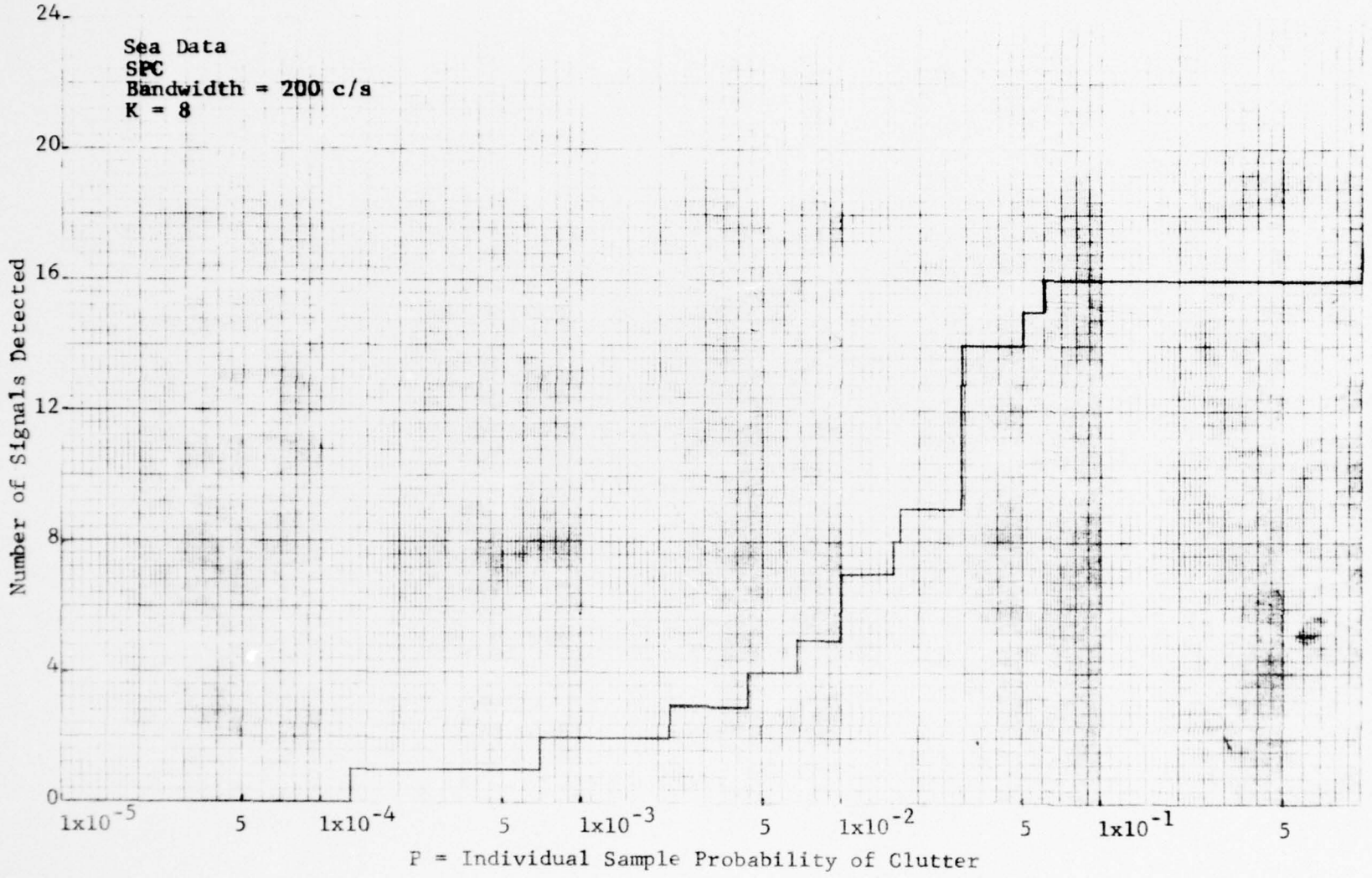

Figure 34 DETECTION STATISTICS: SPC

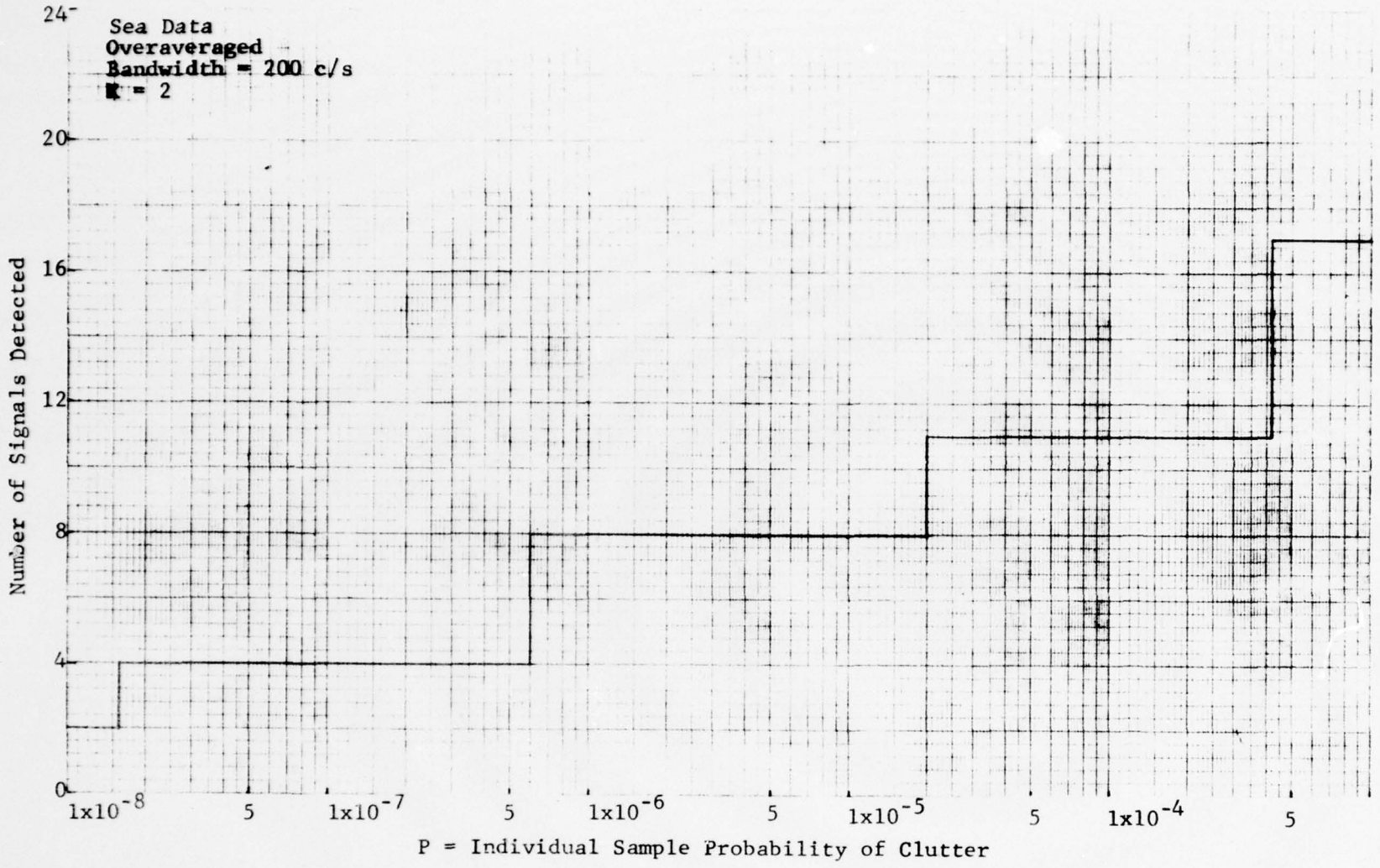

Figure 35 DETECTION STATISTICS: OVERAVERAGED LINEAR CORRELATOR

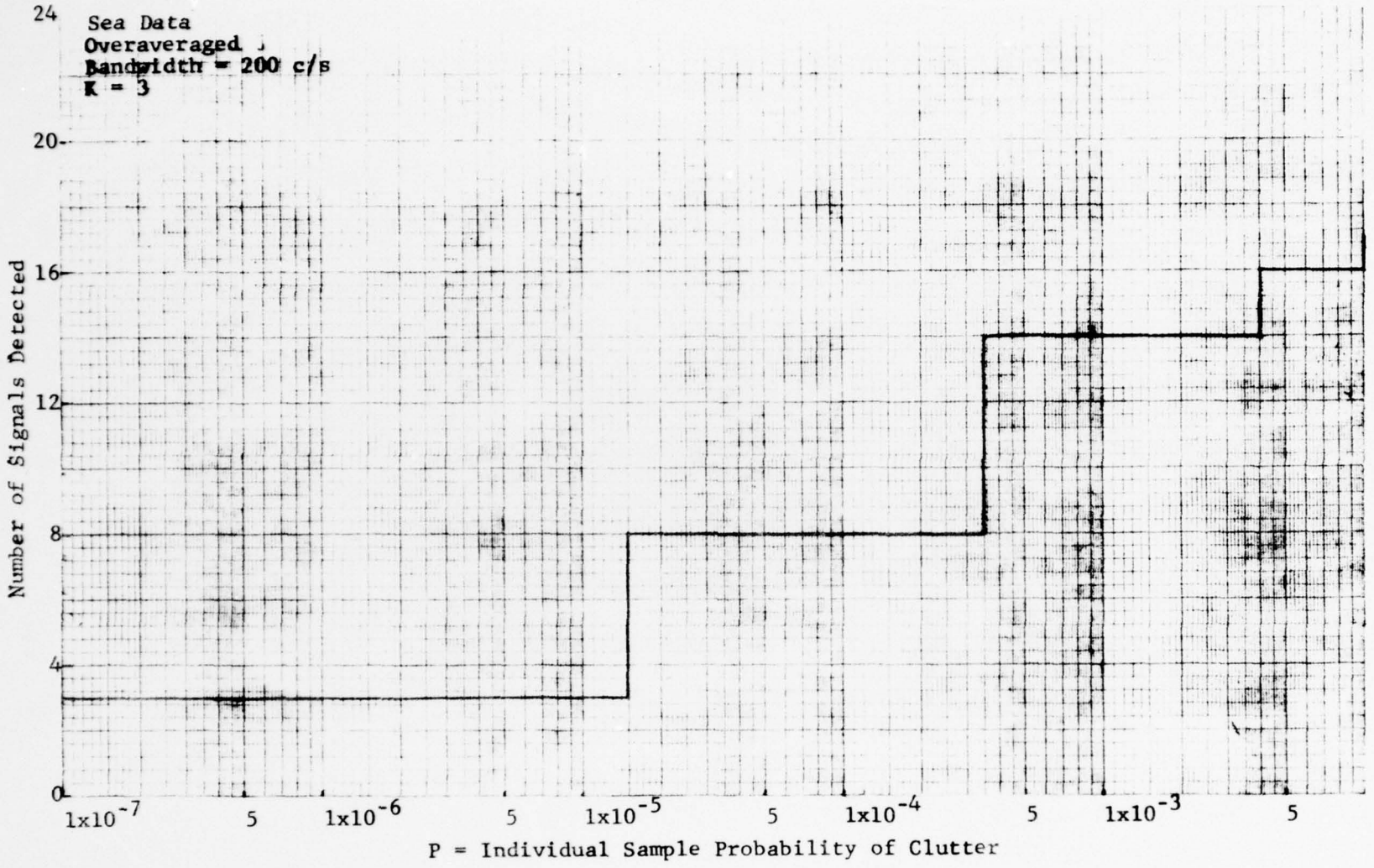

Figure 36 DETECTION STATISTICS: OVERAVERAGED LINEAR CORRELATOR

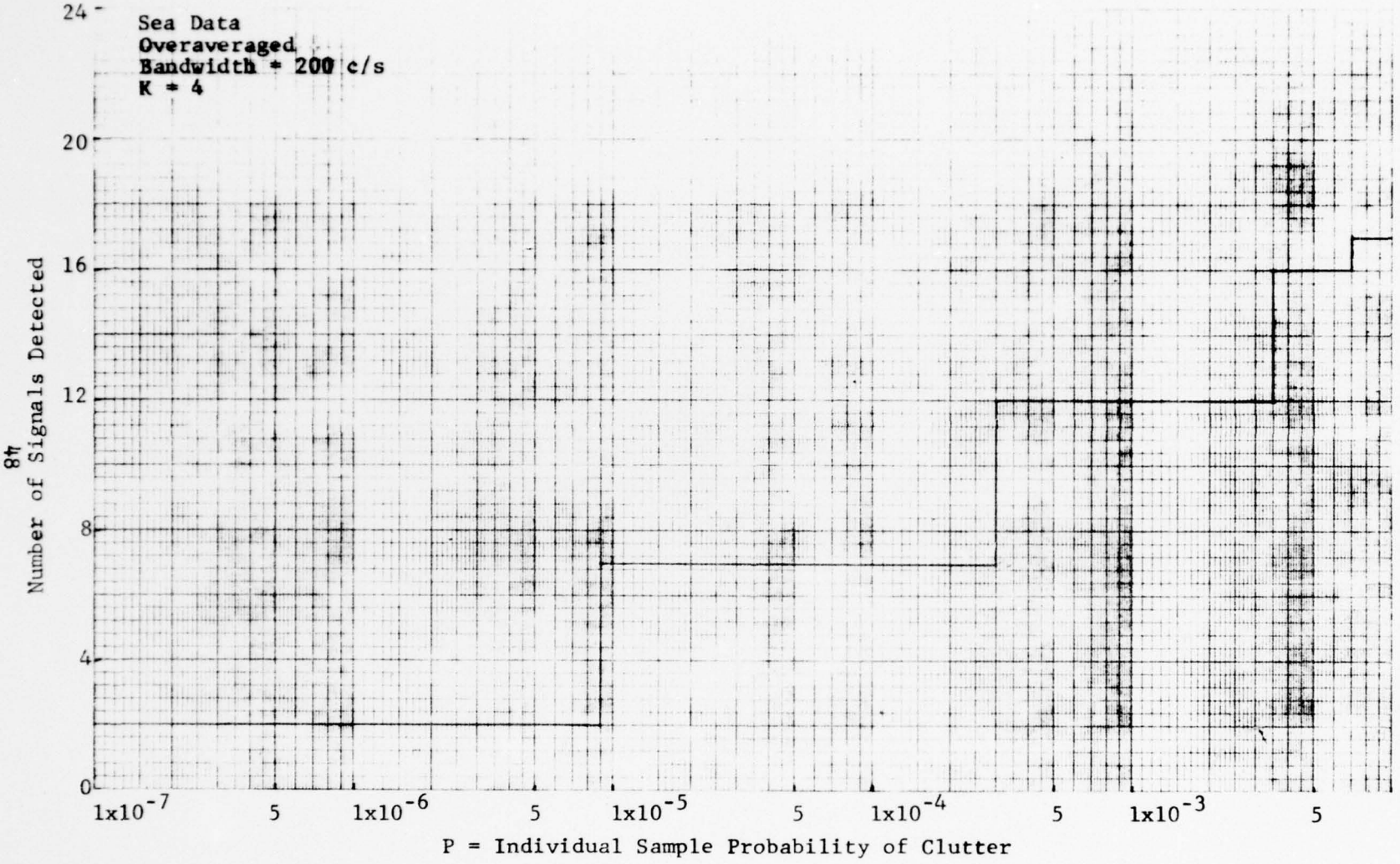

Figure 37 DETECTION STATISTICS: OVERAVERAGED LINEAR CORRELATOR

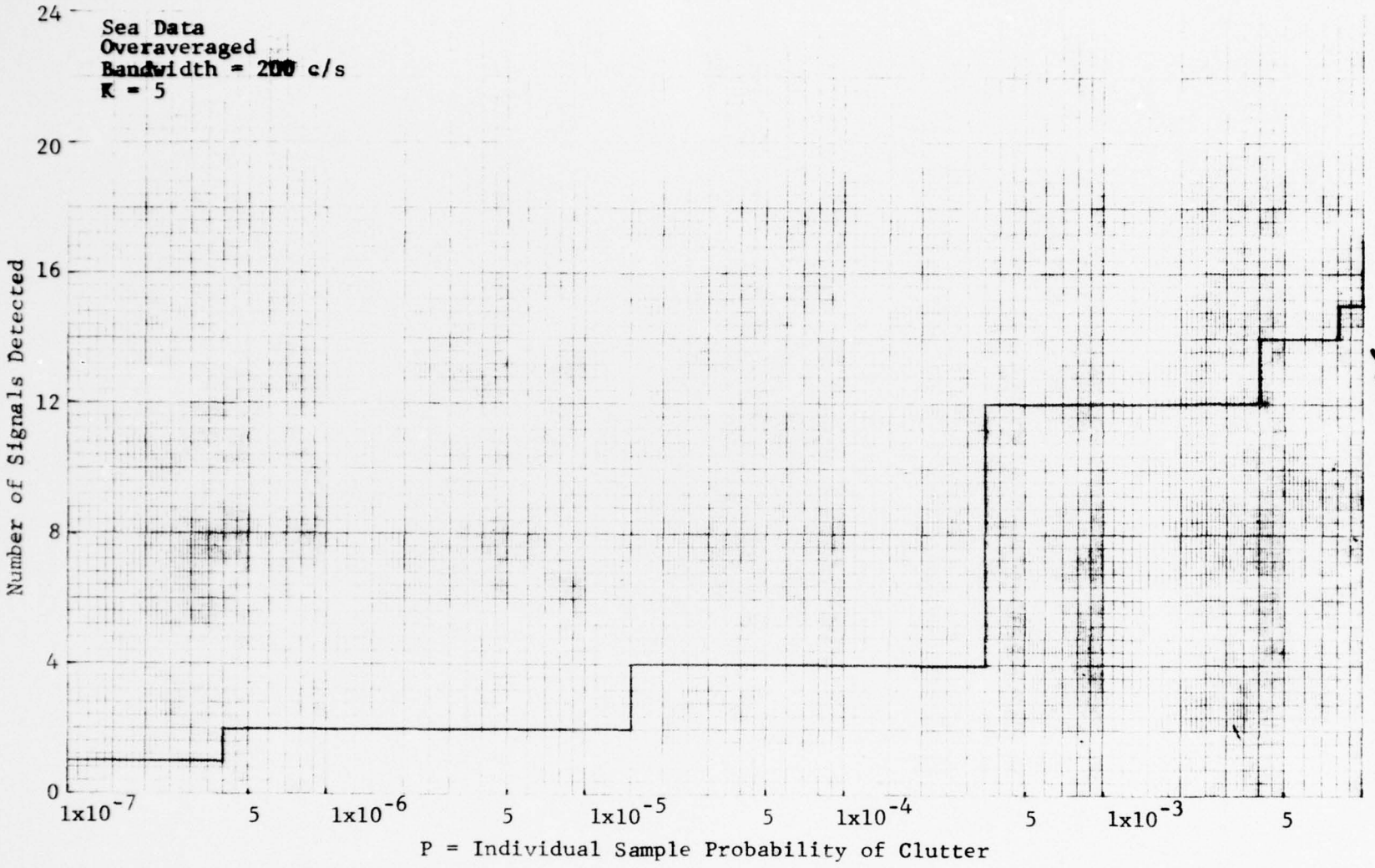

Figure 38 DETECTION STATISTICS: OVERAVERAGED LINEAR CORRELATOR